CP-Violating Effects in Neutralino Scattering and Annihilation

Paolo Gondolo[1*] and Katherine Freese[1,2†]

[1]*Max Planck Institut für Physik, Föhringer Ring 6, 80805 München, Germany*
[2]*Physics Department, University of Michigan, Ann Arbor, MI 48109, USA*

Abstract

We show that in some regions of supersymmetric parameter space, CP violating effects that mix the CP-even and CP-odd Higgs bosons can enhance the neutralino annihilation rate, and hence the indirect detection rate of neutralino dark matter, by factors of 10^6. The same CP violating effects can reduce the neutralino scattering rate off nucleons, and hence the direct detection rate of neutralino dark matter, by factors of 10^{-7}. We study the dependence of these effects on the phase of the trilinear coupling A, and find cases in the region being probed by dark matter searches which are experimentally excluded when CP is conserved but are allowed when CP is violated.

I. INTRODUCTION

The nature of the dark matter in the universe is one of the outstanding questions in astro/particle physics. One of the favored candidates is the lightest supersymmetric (SUSY) particle. Such a particle is weakly interacting and massive (with mass in the range 1 GeV – few TeV), and hence is frequently characterized as a WIMP (weakly interacting massive particle). In the minimal supersymmetric standard model (MSSM), the lightest SUSY particle in most cases is the lightest neutralino, a linear combination of the supersymmetric partners of the photon, Z^0 boson, and neutral-Higgs bosons,

$$\tilde{\chi}_1^0 = N_{11}\widetilde{B} + N_{12}\widetilde{W}^3 + N_{13}\widetilde{H}_1^0 + N_{14}\widetilde{H}_2^0 \tag{1}$$

where $\widetilde{B}$ and $\widetilde{W}^3$ are the supersymmetric partners of the U(1) gauge field B and of the third component of the SU(2) gauge field W^3 that mix to make the photon and Z^0 boson. (We will also use the letter χ for $\tilde{\chi}_1^0$.)

Much work has been done studying the possibilities for detecting these particles. Possibilities include direct detection [1], whereby the particle interacts with a nucleon in a low temperature detector, and is identified by the keV of energy it deposits in the nucleon; and

---

*Email: gondolo@mppmu.mpg.de

†Email: ktfreese@umich.edu

indirect detection, whereby (1) the particles are captured in the Sun or Earth, sink to the center of the Sun or Earth, annihilate with one another in the core, and give rise to particles including neutrinos which can be detected by experiments on the surface of the Earth [2], or (2) the particles annihilate in the galactic halo and produced anomalous components in the flux of cosmic rays [3]. The interaction processes of the lightest SUSY particle are clearly of great importance in calculations of predicted rates for both direct and indirect detection.

In this paper we discuss the effect of CP violation on the neutralino annihilation and scattering cross sections. The MSSM introduces several new phases in the theory which are absent in the standard model. Supplemented by a universality condition at the grand unification scale, only two of these are independent. In this case, one may choose to work in a basis in which the two non-trivial CP-violating phases reside in μ and the universal soft trilinear coupling A of the Higgs fields to the scalar fermions $\tilde{f}$. Previously Falk, Ferstl and Olive [4] have considered the effect on neutralino cross sections of a nonzero phase of μ, the mixing mass parameter involving the two Higgs chiral superfields in the superpotential. Here, on the other hand, we consider the effect on neutralino cross sections of the case where the soft trilinear scalar couplings A_f are all complex numbers, where subscript f refers to the quarks. To be specific, we will take $A \equiv A_t = A_b$ with arbitrary $\arg(A)$, and we take $\mathrm{Im}(\mu) = 0$. In part of SUSY parameter space we find enhancement of these cross sections, and hence an increase in direct and indirect detection rates; while in other parts of parameter space the cross sections are suppressed.

The phase of A enters into the neutralino cross sections in two places: 1) into the squark masses, and 2) into the Higgs sector. For example, one of the processes that contributes to neutralino annihilation is s-channel exchange of the three neutral Higgs bosons, h, H, and A, into final state fermions. (see fig. 1). The first two of these neutral Higgs bosons, h and H, are CP even, while A is CP odd. The new aspect considered here is the possibility of mixing between the CP-even Higgs scalars (h and H) and the CP-odd scalar A. This mixing was first studied by Pilaftsis [5], who found that the size of CP violation can be fairly large, i.e. of order one, for a range of kinematic parameters preferred by SUSY. He found that a large HA mixing can naturally occur within two-Higgs doublet models either at the tree level, if one adds softly CP-violating breaking terms to the Higgs potential, or at one loop, after integrating out heavy degrees of freedom that break the CP invariance of the Higgs sector, such as heavy Majorana neutrinos. In any case, in this paper, we consider the one-loop effects of $\mathrm{Im}(A) \neq 0$ on scattering and annihilation cross sections relevant to direct and indirect detection.

In Section II we discuss our general approach. In Section III, we discuss the squark sector, and in Section IV, the Higgs sector. In Section V, we discuss experimental constraints on the parameters. We present our results in Section VI.

II. GENERAL APPROACH

The minimal supersymmetric standard model provides a well-defined calculational framework [6], but contains at least 106 yet-unmeasured parameters [7]. Most of them control details of the squark and slepton sectors, and can safely be disregarded in dark matter studies. So similarly to Bergström and Gondolo [8], we restrict the number of parameters

to 6 plus one CP violating phase: the "CP-odd" scalar mass m_A (which in our CP violating scenario is just a mass parameter), the Higgs mass parameter μ, the gaugino mass parameter M_2 (we impose gaugino mass unification), the ratio of Higgs vacuum expectation values $\tan\beta$, a sfermion mass parameter $\widetilde{M}$ (not to be confused with the sfermion mass, see eqs. (3) and (6) below), and a complex sfermion mixing parameter $A \equiv A_t = A_b$ for the third generation (we set the A's of the first two generations to zero). The phase of A is the only CP violating phase we introduce besides the standard model CKM phase.

We use the database of points in parameter space built in refs. [8–10], setting their A_b equal to A_t. Hence we explore a substantial fraction of the supersymmetry parameter space, running through different possible neutralinos as the lightest SUSY particle.

We modify the squark and Higgs couplings in the neutralino dark matter code DarkSUSY [11] to include a non-zero phase of A. We also add all diagrams that contribute to neutralino scattering and annihilation and would vanish when CP is conserved.

To investigate the effects of the phase of A, we perform the following procedure. For each of the 132,887 sets of parameter values in the database, we run through 50 values of the phase of A, so that we effectively explore $50 \times 132,887 \sim 6.6 \times 10^6$ models. We loop over a circle with $\arg(A)$ varying from 0 to 2π. At each point, we check bounds on the electric dipole moment, on the Higgs mass, on other particle masses, on the $b \to s\gamma$ branching ratio, and on the invisible Z width (table I gives a listing of the bounds we apply). If any of these bounds are violated, we move to the next point on the circle. If all the bounds are satisfied, we calculate the spin-independent neutralino–proton scattering cross section $\sigma_{\chi p}$. We record the two values of the phase of A where $\sigma_{\chi p}$ is highest and lowest, respectively, with the bounds satisfied. Then, once we have looped through all the possible values for the phase of A, we have found the two points with the maximum enhancement and suppression of the scattering cross section. We then compare with the scattering cross section in the case of no CP violation.

We do the same for the annihilation cross section times relative velocity σv at relative velocity $v = 0$ (we recall that $\sigma \sim 1/v$ as $v \to 0$). Thus we obtain the values of the phase of A where σv is maximum and minimum.

III. SQUARK SECTOR

The (complex) scalar top and bottom mass matrices can be expressed in the $(\tilde{q}_L, \tilde{q}_R)$ basis as

$$\mathcal{M}_{\tilde{q}}^2 = \begin{pmatrix} M_{\tilde{Q}}^2 + m_q^2 + \left(T_{3q} - e_q \sin^2\theta_W\right)\cos 2\beta m_Z^2 & m_q\left(A_q^* - \mu R_q\right) \\ m_q\left(A_q - \mu^* R_q\right) & M_{\tilde{R}}^2 + m_q^2 + e_q \sin^2\theta_W m_Z^2 \cos 2\beta \end{pmatrix}, \quad (2)$$

where $q = t$ or b; $e_t = \frac{2}{3}$; $e_b = -\frac{1}{3}$; $T_{3t} = \frac{1}{2}$; $T_{3b} = -\frac{1}{2}$; $R_t = \cot\beta$, $R_b = \tan\beta$; and $M_{\tilde{R}}^2 = M_{\tilde{U}}^2$ $[M_{\tilde{D}}^2]$ for t $[b]$. We set

$$M_{\tilde{Q}} = M_{\tilde{U}} = M_{\tilde{D}} = \widetilde{M}, \quad (3)$$

our sfermion mass parameter. Even in the case of no CP violation, when both μ and A are real, there is mixing between the squarks, and this matrix must be diagonalized to find the

3

mass eigenstates. Here we take A to be complex. Then we obtain the mass eigenstates $\tilde{q}_1, \tilde{q}_2$ from the weak eigenstates $\tilde{q}_L, \tilde{q}_R$ through the rotation

$$
\begin{pmatrix} \tilde{q}_1 \\ \tilde{q}_2 \end{pmatrix} = \begin{pmatrix} \cos\theta_{\tilde{q}} & \sin\theta_{\tilde{q}}e^{i\gamma_{\tilde{q}}} \\ -\sin\theta_{\tilde{q}} & \cos\theta_{\tilde{q}}e^{i\gamma_{\tilde{q}}} \end{pmatrix} \begin{pmatrix} \tilde{q}_L \\ \tilde{q}_R \end{pmatrix}, \tag{4}
$$

where $\gamma_{\tilde{q}} = \arg(A_q^* - \mu R_q)$ and the rotation angle $\theta_{\tilde{q}}$ $(-\pi/4 \leq \theta_{\tilde{q}} \leq \pi/4)$ may be obtained by

$$
\tan(2\theta_{\tilde{q}}) = \frac{2m_q|A_q^* - \mu R_q|}{M_{\tilde{R}}^2 - M_{\tilde{Q}}^2 + (2e_q\sin^2\theta_W - T_{3q})m_Z^2\cos 2\beta}. \tag{5}
$$

The masses of $\tilde{q}_1$ and $\tilde{q}_2$ are then given by

$$
\begin{aligned}
m_{\tilde{q}_{1,2}}^2 = \frac{1}{2}\bigg\{ & M_{\tilde{Q}}^2 + M_{\tilde{R}}^2 + T_{3q}m_Z^2\cos 2\beta \\
& \pm \mathrm{sign}(\theta_{\tilde{q}})\sqrt{\left[M_{\tilde{R}}^2 - M_{\tilde{Q}}^2 + (2e_q\sin^2\theta_W - T_{3q})m_Z^2\cos 2\beta\right]^2 + 4m_q^2\left|A_q^* - \mu R_q\right|^2}\bigg\}. \tag{6}
\end{aligned}
$$

The $+$ sign is for $\tilde{q}_1$ and the $-$ sign for $\tilde{q}_2$.

The mixing in eq. (4) also modifies the squark couplings to the neutralino and the corresponding quark. Writing the relevant interaction term as

$$
\mathcal{L}_{\mathrm{int}} = \tilde{q}_i\overline{\chi}\left(g_{\tilde{q}_i\chi q}^L P_L + g_{\tilde{q}_i\chi q}^R P_R\right)q + \mathrm{h.c.}, \tag{7}
$$

with $P_L = (1 - \gamma_5)/2$, $P_R = (1 + \gamma_5)/2$, and $i = 1, 2$, we have

$$
\begin{pmatrix} g_{\tilde{q}_1\chi q}^K \\ g_{\tilde{q}_2\chi q}^K \end{pmatrix} = \begin{pmatrix} \cos\theta_{\tilde{q}} & \sin\theta_{\tilde{q}}e^{i\gamma_{\tilde{q}}} \\ -\sin\theta_{\tilde{q}} & \cos\theta_{\tilde{q}}e^{i\gamma_{\tilde{q}}} \end{pmatrix} \begin{pmatrix} g_{KL} \\ g_{KR} \end{pmatrix} \tag{8}
$$

where $K = L, R$,

$$
g_{LL} = -\sqrt{2}\left(T_{3q}gN_{12} + (e_q - T_{3q})g'N_{11}\right), \qquad g_{RR} = \sqrt{2}e_q g'N_{11}, \tag{9}
$$

and

$$
g_{LR} = g_{RL} = -\frac{gm_u N_{14}}{\sqrt{2}m_W\sin\beta} \tag{10}
$$

for the up-type quarks,

$$
g_{LR} = g_{RL} = -\frac{gm_d N_{13}}{\sqrt{2}m_W\cos\beta} \tag{11}
$$

for the down-type quarks.

The expressions in this section apply to sleptons provided up-type (s)quarks is replaced with (s)neutrinos and down-type (s)quarks with charged (s)leptons.

IV. HIGGS SECTOR

A. Higgs masses

We evaluate the Higgs boson masses in the effective potential approach. The radiatively corrected Higgs boson mass matrix can be written as

$$\mathcal{M}^2 = \begin{pmatrix} m_Z^2 \cos^2\beta + m_A^2 \sin^2\beta + \Delta_{11} & -(m_A^2 + m_Z^2)\sin\beta\cos\beta + \Delta_{12} & \Delta_{13} \\ -(m_A^2 + m_Z^2)\sin\beta\cos\beta + \Delta_{21} & m_Z^2 \sin^2\beta + m_A^2 \cos^2\beta + \Delta_{22} & \Delta_{23} \\ \Delta_{31} & \Delta_{32} & m_A^2 \end{pmatrix} \quad (12)$$

in the basis H_1, H_2, H_3. Here $\Delta_{ij} = \Delta_{ji}$ are the radiative corrections coming from quark and squark loops, with Δ_{13} and Δ_{23} arising from CP violation. We take Δ_{11}, Δ_{12}, and Δ_{22} from ref. [12].

$$\Delta_{11} = \frac{3g^2}{16\pi^2 m_W^2}\left[\frac{m_b^4}{\cos^2\beta}\left(\ln\frac{m_{\tilde{b}_1}^2 m_{\tilde{b}_2}^2}{m_b^4} + 2Z_b \ln\frac{m_{\tilde{b}_1}^2}{m_{\tilde{b}_2}^2}\right)\right.$$
$$\left. + \frac{m_b^4}{\cos^2\beta}Z_b^2 g(m_{\tilde{b}_1}^2, m_{\tilde{b}_2}^2) + \frac{m_t^4}{\sin^2\beta}W_t^2 g(m_{\tilde{t}_1}^2, m_{\tilde{t}_2}^2)\right], \quad (13)$$

$$\Delta_{22} = \frac{3g^2}{16\pi^2 m_W^2}\left[\frac{m_t^4}{\sin^2\beta}\left(\ln\frac{m_{\tilde{t}_1}^2 m_{\tilde{t}_2}^2}{m_t^4} + 2Z_t \ln\frac{m_{\tilde{t}_1}^2}{m_{\tilde{t}_2}^2}\right)\right.$$
$$\left. + \frac{m_t^4}{\sin^2\beta}Z_t^2 g(m_{\tilde{t}_1}^2, m_{\tilde{t}_2}^2) + \frac{m_b^4}{\sin^2\beta}W_b^2 g(m_{\tilde{b}_1}^2, m_{\tilde{b}_2}^2)\right], \quad (14)$$

$$\Delta_{12} = \frac{3g^2}{16\pi^2 m_W^2}\left[\frac{m_t^4}{\sin^2\beta}W_t\left(\ln\frac{m_{\tilde{t}_1}^2}{m_{\tilde{t}_2}^2} + Z_t g(m_{\tilde{t}_1}^2, m_{\tilde{t}_2}^2)\right)\right.$$
$$\left. + \frac{m_b^4}{\cos^2\beta}W_b\left(\ln\frac{m_{\tilde{b}_1}^2}{m_{\tilde{b}_2}^2} + Z_b g(m_{\tilde{b}_1}^2, m_{\tilde{b}_2}^2)\right)\right], \quad (15)$$

where

$$W_q = \frac{\text{Re}(\mu A_q) - |\mu|^2 R_q}{m_{\tilde{q}_2}^2 - m_{\tilde{q}_1}^2}, \quad (16)$$

$$Z_q = \frac{|A_q|^2 - \text{Re}(\mu A_q)R_q}{m_{\tilde{q}_2}^2 - m_{\tilde{q}_1}^2}, \quad (17)$$

$$g(m_1^2, m_2^2) = 2 - \frac{m_1^2 + m_2^2}{m_1^2 - m_2^2}\ln\frac{m_1^2}{m_2^2}. \quad (18)$$

We have rewritten Δ_{13} and Δ_{23} from ref. [5] in a way that shows their proportionality to $\text{Im}(\mu A)$.

$$\Delta_{k3} = \frac{3}{16\pi^2}\sum_q g_{A\tilde{q}_1\tilde{q}_1}\left\{\frac{1}{2}\left(g_{H_k\tilde{q}_L\tilde{q}_L} + g_{H_k\tilde{q}_R\tilde{q}_R}\right)\log\frac{m_{\tilde{q}_1}^2}{m_{\tilde{q}_2}^2}\right. \quad (19)$$

$$\left. + \left[\sin 2\theta_q \text{Re}(e^{i\gamma_q}g_{H_k\tilde{q}_R\tilde{q}_L}) + \frac{1}{2}\cos 2\theta_q\left(g_{H_k\tilde{q}_L\tilde{q}_L} - g_{H_k\tilde{q}_R\tilde{q}_R}\right)\right]g\left(m_{\tilde{q}_1}^2, m_{\tilde{q}_1}^2\right)\right\}, \quad (20)$$

where the couplings of the Higgs bosons to the squarks are

$$g_{A\tilde{t}_1\tilde{t}_1} = -\frac{gm_t^2}{m_W \sin^2 \beta} \frac{\mathrm{Im}(\mu A_t)}{m_{\tilde{t}_1}^2 - m_{\tilde{t}_2}^2}, \tag{21}$$

$$g_{A\tilde{b}_1\tilde{b}_1} = -\frac{gm_b^2}{m_W \cos^2 \beta} \frac{\mathrm{Im}(\mu A_b)}{m_{\tilde{b}_1}^2 - m_{\tilde{b}_2}^2}, \tag{22}$$

$$g_{H_1\tilde{t}_L\tilde{t}_L} = -\frac{gm_Z}{\cos \theta_W} \left(T_{3t} - e_t \sin^2 \theta_W \right) \cos \beta, \tag{23}$$

$$g_{H_1\tilde{t}_R\tilde{t}_R} = -\frac{gm_Z}{\cos \theta_W} e_t \sin^2 \theta_W \cos \beta, \tag{24}$$

$$g_{H_1\tilde{t}_R\tilde{t}_L} = \frac{gm_t\mu^*}{2m_W \sin \beta}, \tag{25}$$

$$g_{H_1\tilde{b}_L\tilde{b}_L} = -\frac{gm_b^2}{m_W \cos \beta} - \frac{gm_Z}{\cos \theta_W} \left(T_{3b} - e_b \sin^2 \theta_W \right) \cos \beta, \tag{26}$$

$$g_{H_1\tilde{b}_R\tilde{b}_R} = -\frac{gm_b^2}{m_W \cos \beta} - \frac{gm_Z}{\cos \theta_W} e_b \sin^2 \theta_W \cos \beta, \tag{27}$$

$$g_{H_1\tilde{b}_R\tilde{b}_L} = -\frac{gm_b A_b}{2m_W \cos \beta}, \tag{28}$$

$$g_{H_2\tilde{t}_L\tilde{t}_L} = -\frac{gm_{b^2}}{m_W \cos \beta} + \frac{gm_Z}{\cos \theta_W} \left(T_{3t} - e_t \sin^2 \theta_W \right) \sin \beta, \tag{29}$$

$$g_{H_2\tilde{t}_R\tilde{t}_R} = -\frac{gm_b^2}{m_W \cos \beta} + \frac{gm_Z}{\cos \theta_W} e_t \sin^2 \theta_W \sin \beta, \tag{30}$$

$$g_{H_2\tilde{t}_R\tilde{t}_L} = -\frac{gm_t A_t}{2m_W \sin \beta}, \tag{31}$$

$$g_{H_2\tilde{b}_L\tilde{b}_L} = \frac{gm_Z}{\cos \theta_W} \left(T_{3b} - e_b \sin^2 \theta_W \right) \sin \beta, \tag{32}$$

$$g_{H_2\tilde{b}_R\tilde{b}_R} = \frac{gm_z}{\cos \theta_W} e_b \sin^2 \theta_W \sin \beta, \tag{33}$$

$$g_{H_2\tilde{b}_R\tilde{b}_L} = \frac{gm_b\mu^*}{2m_W \cos \beta}. \tag{34}$$

Neglecting D terms, as we should for consistency with the CP even part and the vertices in our effective potential approach, the corrections Δ_{13} and Δ_{23} simplify to

$$\Delta_{13} = \frac{3g^2}{16\pi^2 m_W^2} \left[\frac{m_b^4}{\cos^3 \beta} X_b \left(\ln \frac{m_{\tilde{b}_1}^2}{m_{\tilde{b}_2}^2} + Z_b g(m_{\tilde{b}_1}^2, m_{\tilde{b}_2}^2) \right) \right.$$
$$\left. + \frac{m_t^4}{\sin^3 \beta} X_t W_t \, g(m_{\tilde{t}_1}^2, m_{\tilde{t}_2}^2) \right], \tag{35}$$

$$\Delta_{23} = \frac{3g^2}{16\pi^2 m_W^2} \left[\frac{m_t^4}{\sin^3 \beta} X_t \left(\ln \frac{m_{\tilde{t}_1}^2}{m_{\tilde{t}_2}^2} + Z_t g(m_{\tilde{t}_1}^2, m_{\tilde{t}_2}^2) \right) \right.$$
$$\left. + \frac{m_b^4}{\cos^3 \beta} X_b W_b \, g(m_{\tilde{b}_1}^2, m_{\tilde{b}_2}^2) \right], \tag{36}$$

with

$$X_q = \frac{\text{Im}(\mu A_q)}{m_{\tilde{q}_1}^2 - m_{\tilde{q}_2}^2}. \tag{37}$$

The key thing to notice is that the Δ_{k3} self-energies are proportional to $\text{Im}(\mu A)$. For μ real, they are hence proportional to $\text{Im}(A)$.

We use the effective potential approach to obtain the Higgs masses and couplings. The Higgs mass eigenstates h_i ($i = 1, 2, 3$) are obtained by diagonalizing the Higgs mass matrix including radiative corrections in eq. (12) through the orthogonal Higgs mixing matrix O as

$$H_i = O_{ij} h_j \tag{38}$$

In practice, it is convenient to implement the diagonalization in two steps, to separate the CP violating contributions. First we diagonalize the "CP-even" part through

$$H_i = O_{ij}^0 \Phi_j, \tag{39}$$

where $\Phi_i = H, h, A$ for $i = 1, 2, 3$ respectively. The matrix O^0 would be the Higgs mixing matrix in absence of CP violation

$$O^0 = \begin{pmatrix} \cos\alpha & -\sin\alpha & 0 \\ \sin\alpha & \cos\alpha & 0 \\ 0 & 0 & 1 \end{pmatrix}, \tag{40}$$

with

$$\tan(2\alpha) = \frac{2\mathcal{M}_{12}^2}{\mathcal{M}_{11}^2 - \mathcal{M}_{22}^2}. \tag{41}$$

Then we further rotate to the mass eigenstates with an orthogonal matrix O' as

$$\Phi_i = O'_{ij} h_j \tag{42}$$

with $O' = OO^{0T}$. This two step procedure allows for a rapid introduction of CP violating mixing angles for the Higgs sector in the DarkSUSY code.

B. Higgs couplings

We will include CP violating effects by rotating couplings of Higgs particles to other particles as described in this section. In the effective potential approach we neglect vertex corrections. This incorporates the dominant corrections of $\mathcal{O}(g^2 m_t^4 / m_W^4)$, and neglects corrections of $\mathcal{O}(g^2 m_t^2 / m_W^2)$.

There are terms in the Lagrangian that couple the Higgs particles to other particles that are linear in the Higgs fields, for example

$$g_{\Phi_i q q} \Phi_i \bar{q} q = g_{h_i q q} O'_{ji} h_j \bar{q} q. \tag{43}$$

Terms of this type include coupling to fermions, as shown above, and also terms such as $g_{WH^+\Phi_i} W H^+ \Phi_i$. We will define rotated couplings via

$$g_{h_iab} = O'_{ij}g_{\Phi_jab} \tag{44}$$

where a and b stand for the appropriate particle name.

Those terms with two Higgs bosons in them, such as

$$g_{Z\Phi_3\Phi_i}Z\Phi_3\partial_\mu\Phi_i = g_{Z\Phi_3\Phi_i}O'_{k3}O'_{ji}Zh_k\partial_\mu h_j, \tag{45}$$

must have the couplings rotated with two multiplications by O', e.g.,

$$g_{Zh_kh_j} = g_{ZA\Phi_i}O'_{ji}O'_{k3} - (k \leftrightarrow j). \tag{46}$$

Note that, in this particular term, the appropriate antisymmetry properties are maintained, and i takes on values 1 or 2 only.

We have carefully rotated all couplings involving one, two, or three Higgs bosons. It is these rotated couplings that we use in the numerical code. (i.e. we replace the ordinary Higgs couplings with these rotated couplings.)

As an example, we give the Higgs–quark and Higgs–neutralino vertices that appear in the neutralino–proton spin-independent cross section.

$$g_{h_iuu} = -\frac{gm_u}{2m_W \sin\beta}\left(O'_{i1}\sin\alpha + O'_{i2}\cos\alpha + O'_{i3}i\cos\beta\right), \tag{47}$$

$$g_{h_idd} = -\frac{gm_d}{2m_W \cos\beta}\left(O'_{i1}\cos\alpha - O'_{i2}\sin\alpha + O'_{i3}i\sin\beta\right), \tag{48}$$

$$g_{h_i\chi_m\chi_n} = \frac{1}{2}(gN^*_{m2} - g'N^*_{m1})\left[N^*_{n3}\left(-O'_{i1}\cos\alpha + O'_{i2}\sin\alpha + O'_{i3}i\sin\beta\right) + \right.$$
$$\left. N^*_{n4}\left(O'_{i1}\sin\alpha + O'_{i2}\cos\alpha - O'_{i3}i\cos\beta\right)\right] + (m \leftrightarrow n). \tag{49}$$

Here u stands for down-type quarks and neutrinos, d stands for up-type quarks and charged leptons.

V. EXPERIMENTAL BOUNDS

A. Bounds on masses

We impose experimental bounds on the invisible width of the Z^0 boson, Γ_Z^{inv}, and on particle masses as listed in table I.

Since the h, H, and A are rotated into new mass eigenstates bosons, we use the most model independent constraint on the neutral Higgs masses: we take $m_{h_i} > 82.5$ GeV. This constraint was reported by the ALEPH group [13] at the 95% C.L. as a bound on all Higgs masses, independent of $\sin^2(\beta - \alpha)$. Note that this bound, which is a 10% improvement over previous bounds, renders the cross section for direct detection of SUSY particles smaller by a factor of two. This suppression arises because the dominant contribution to the scattering cross section is via Higgs exchange and scales as $\sigma_{\chi p} \propto 1/m_{h_i}^4$.

B. Bounds on CP violation

We impose bounds on the branching ratio $\mathrm{BR}(b \to s\gamma)$, and on the electric dipole moments of the electron and of the neutron d_e and d_n.

For $\mathrm{BR}(b \to s\gamma)$ we use the expressions in ref. [14], with inclusion of the one-loop QCD corrections.

Since we assume that the only new CP violating phase is that of A, the leading contribution to the electric dipole moment (EDM) arises at two-loops [15]. Chang, Keung, and Pilaftsis [15] have calculated two-loop contributions to the electric dipole moment (EDM) which originate from the potential CP violation due to a nonzero phase of A. We rewrite them showing explicitly their dependence on $\mathrm{Im}(\mu A)$. They find the electric and chromo-electric EDM of a light fermion f at the electroweak scale as

$$(d_f^E)_{EW} = e e_f \frac{3\alpha_{\mathrm{em}}}{64\pi^3} \frac{R_f m_f}{m_A^2} \sum_{q=t,b} \xi_q e_q^2 \left[F\left(\frac{m_{\tilde{q}_1}^2}{m_A^2}\right) - F\left(\frac{m_{\tilde{q}_2}^2}{m_A^2}\right) \right], \tag{50}$$

$$(d_f^C)_{EW} = g_s e_f \frac{\alpha_s}{128\pi^3} \frac{R_f m_f}{m_A^2} \sum_{q=t,b} \xi_q \left[F\left(\frac{m_{\tilde{q}_1}^2}{m_A^2}\right) - F\left(\frac{m_{\tilde{q}_2}^2}{m_A^2}\right) \right], \tag{51}$$

where $\alpha_{\mathrm{em}} = e^2/(4\pi)$ is the electromagnetic fine structure constant, $\alpha_s = g_s^2/(4\pi)$ is the strong coupling constant, all the kinematic parameters must be evaluated at the electroweak scale m_Z, e_i is the electric charge of particle i, $R_f = \tan\beta$ for $f = u, c, t$, $R_f = \cot\beta$ for $f = e, \mu, \tau, d, s, b$, and $F(z)$ is a two-loop function given by

$$F(z) = \int_0^1 dx \frac{x(1-x)}{z - x(1-x)} \ln\left[\frac{x(1-x)}{z}\right]. \tag{52}$$

The EDM of the neutron can then be estimated by a naive dimensional analysis [16,17] as

$$d_n = \eta^E \frac{1}{3}\left(4d_d^E - d_u^E\right) + \eta^C \frac{e}{12\pi}\left(4d_d^C - d_u^C\right). \tag{53}$$

We take the numerical values $\eta^E = 1.53$ and $\eta^C = 3.4$ [17].

The CP violating quantities ξ_t and ξ_b are given by

$$\xi_t = -\frac{g m_t^3 \, \mathrm{Im}(\mu A_t)}{2 m_W^2 \sin^2\beta (m_{\tilde{t}_1}^2 - m_{\tilde{t}_2}^2)} \tag{54}$$

and

$$\xi_b = -\frac{g m_b^3 \, \mathrm{Im}(\mu A_b)}{2 m_W^2 \cos^2\beta (m_{\tilde{b}_1}^2 - m_{\tilde{b}_2}^2)}. \tag{55}$$

As an upper bound to the contribution to the measured value of the electron EDM we take $|d_e| < 0.4 \times 10^{-26} ecm$ [18]. The bound on the neutron EDM is $|d_n| < 1.79 \times 10^{-25} ecm$ [19]. We keep only models that satisfy these bounds.

9

VI. SCATTERING CROSS SECTION

The neutralino–proton scattering cross section for spin-independent interactions can be written as

$$\sigma_{\chi p} = \frac{G_{\chi p}^2 \mu_{\chi p}^2}{\pi}, \tag{56}$$

where $\mu_{\chi p} = m_\chi m_p / (m_\chi + m_p)$ is the reduced neutralino–proton mass, and

$$G_{\chi p} = \sum_q \frac{f_q m_p}{m_q} \left[\sum_{i=1}^3 \frac{\mathrm{Re}(g_{h_i \chi\chi}) \, \mathrm{Re}(g_{h_i qq})}{m_{h_i}^2} - \frac{1}{2} \sum_{k=1}^2 \frac{\mathrm{Re}(g_{\tilde{q}_k \chi q}^L g_{\tilde{q}_k \chi q}^{R*})}{m_{\tilde{q}_k}^2} \right]. \tag{57}$$

The sum over q runs over all quarks. The coupling constants are given in eqs. (8,47–49). We take [35]

$$f_u = 0.023, \quad f_d = 0.034, \quad f_s = 0.14, \quad f_c = f_b = f_t = 0.0595, \tag{58}$$

and

$$\begin{aligned} m_u &= 5.6\mathrm{MeV}, \quad m_d = 9.9\mathrm{MeV}, \quad m_s = 199\mathrm{MeV}, \\ m_c &= 1.35\mathrm{GeV}, \quad m_b = 5\mathrm{GeV}, \quad m_t = 175\mathrm{GeV}. \end{aligned} \tag{59}$$

Notice that only the real part of the couplings of the Higgs and neutralinos to Higgs bosons in eq. (47–49) enter the scattering cross section. Since both g_{Aqq} and $g_{A\chi\chi}$ are purely imaginary (because $\mathrm{Im}(\mu) = 0$), introducing a phase in A cannot possibly enhance the Higgs couplings in eq. (57). Similarly, the neutralino–squark–quark couplings can only be suppressed for $\mathrm{Im}(A) \neq 0$. However, enhancements to the scattering cross section can still come from the Higgs or squark masses in the denominator in eq. (57).

VII. ANNIHILATION CROSS SECTION

The neutralino–neutralino annihilation cross section times relative velocity σv is relevant for neutralino annihilations in the center of the Earth and Sun and in the galactic halo. An enhancement in σv may lead to a higher annihilation signal from the Earth when the capture of neutralinos in the core has not yet reached equilibrium with their self–annihilation. An increased σv gives directly an increased intensity of positron, antiproton, and gamma-ray fluxes from neutralino annihilation in the galactic halo.

The neutralino annihilation cross section also determines the relic density of neutralinos. In this case, there are important contributions at $v \neq 0$ (p-waves, etc.) in large regions of the supersymmetric parameter space. Due to the excessive computational cost of obtaining the relic density in presence of CP violation, in this paper we consider only the $v = 0$ case, and postpone the study of the effect of CP violating phases on the neutralino relic density. The enhancements and suppressions of σv at $v = 0$ that we obtain in the following are indications of analogous enhancements and suppressions in the neutralino relic density.

The annihilation cross section at $v = 0$ includes the following contributions

$$\sigma v = \left[\sum_f \sigma_{\overline{f}f} + \sigma_{W^+W^-} + \sigma_{ZZ} + \sigma_{H^+W^-} + \sigma_{H^-W^+} + \sum_{i=1}^{3} \sigma_{h_i Z} + \sum_{ij=1}^{3} \sigma_{h_i h_j} \right] v \qquad (60)$$

where σ_{XY} refers to the annihilation channel $\chi\chi \to XY$, which is open when $2m_\chi \geq m_X + m_Y$.

The annihilation cross section in each channel can be written in terms of helicity amplitudes $\mathcal{A}$ as

$$\sigma_{XY} v = \frac{\lambda_{XY}}{128\pi m_\chi^2} \sum_{\text{helicities}} \left| \mathcal{A} \right|^2 \qquad (61)$$

where the amplitudes are normalized as in ref. [20] and

$$\lambda_{XY} = \sqrt{\left[1 - \frac{(m_X + m_Y)^2}{4m_\chi^2} \right] \left[1 - \frac{(m_X - m_Y)^2}{4m_\chi^2} \right]}. \qquad (62)$$

The DarkSUSY code already includes analytic expressions for each helicity amplitude required in eq. (61), with arbitrary complex couplings between the particles. Hence once we have rotated all vertices as described in sect. IV, and have added all annihilation diagrams that vanish when CP is conserved (e.g. the s-channel exchange of all Higgs bosons), the annihilation cross section including CP violation is automatically calculated correctly by DarkSUSY.

For future reference, we list the individual contributions to the annihilation cross section including terms that violate CP.

$$\sigma_{\overline{f}f} v = \frac{N_f \lambda_{ff} m_\chi^2}{32\pi} \left| \sum_{i=1}^{3} \frac{4\,\mathrm{Im}(g_{h_i ff})\,\mathrm{Im}(g_{h_i \chi_1 \chi_1})}{m_{h_i}^2 - 4m_\chi^2 - im_{h_i}\Gamma_{h_i}} + \frac{4g_{Zff}^A\,\mathrm{Re}(g_{Z\chi_1\chi_1})(m_f/m_\chi)}{m_Z^2} + \right.$$
$$\left. + \sum_{s=1}^{2} \frac{(|g_{\tilde{f}_s \chi f}^R|^2 + |g_{\tilde{f}_s \chi f}^L|^2)(m_f/m_\chi) + 2\,\mathrm{Re}(g_{\tilde{f}_s \chi f}^L g_{\tilde{f}_s \chi f}^{R*})}{m_{\tilde{f}_s}^2 + m_\chi^2 - m_f^2 - im_{\tilde{f}_s}\Gamma_{\tilde{f}_s}} \right|^2 +$$
$$+ \frac{N_f \lambda_{ff}^3 m_\chi^2}{32\pi} \left| \sum_{i=1}^{3} \frac{4i\,\mathrm{Re}(g_{h_i ff})\,\mathrm{Im}(g_{h_i \chi_1 \chi_1})}{m_{h_i}^2 - 4m_\chi^2 - im_{h_i}\Gamma_{h_i}} + \sum_{s=1}^{2} \frac{|g_{\tilde{f}_s \chi f}^R|^2 - |g_{\tilde{f}_s \chi f}^L|^2}{m_{\tilde{f}_s}^2 + m_\chi^2 - m_f^2 - im_{\tilde{f}_s}\Gamma_{\tilde{f}_s}} \right|^2, \qquad (63)$$

$$\sigma_{W^+W^-} v = \frac{\lambda_{WW}}{8\pi} \left| \sum_{c=1}^{2} \frac{\lambda_{WW} m_\chi (|g_{W\chi\tilde{\chi}_c^+}^R|^2 + |g_{W\chi\tilde{\chi}_c^+}^L|^2) + 2im_{\tilde{\chi}_c^+}\,\mathrm{Im}(g_{W\chi\tilde{\chi}_c^+}^L g_{W\chi\tilde{\chi}_c^+}^{R*})}{m_{\tilde{\chi}_c^+}^2 + m_\chi^2 - m_W^2 - im_{\tilde{\chi}_c^+}\Gamma_{\tilde{\chi}_c^+}} \right|^2 +$$
$$+ \frac{\lambda_{WW}}{4\pi} \left| \sum_{c=1}^{2} \frac{[2(m_\chi/m_W)^2 - 1]m_{\tilde{\chi}_c^+}\,\mathrm{Im}(g_{W\chi\tilde{\chi}_c^+}^L g_{W\chi\tilde{\chi}_c^+}^{R*})}{m_{\tilde{\chi}_c^+}^2 + m_\chi^2 - m_W^2 - im_{\tilde{\chi}_c^+}\Gamma_{\tilde{\chi}_c^+}} \right|^2, \qquad (64)$$

$$\sigma_{ZZ} v = \frac{\lambda_{WW}}{16\pi} \left| \sum_{n=1}^{4} \frac{2\lambda_{ZZ} m_\chi |g_{Z\chi\chi_n}|^2 - 2im_{\chi_n}\,\mathrm{Im}(g_{Z\chi\chi_n}^2)}{m_{\chi_n}^2 + m_\chi^2 - m_Z^2 - im_{\chi_n}\Gamma_{\chi_n}} \right|^2 +$$
$$+ \frac{\lambda_{WW}}{8\pi} \left| \sum_{n=1}^{4} \frac{[2(m_\chi/m_W)^2 - 1]m_{\chi_n}\,\mathrm{Im}(g_{Z\chi\chi_n}^2)}{m_{\chi_n}^2 + m_\chi^2 - m_Z^2 - im_{\chi_n}\Gamma_{\chi_n}} \right|^2, \qquad (65)$$

$$\sigma_{H^+W^-} v = \sigma_{H^-W^+} v = \frac{\lambda_{H^\pm W}^3 m_\chi^2}{16\pi m_W^2} \left| \sum_{i=1}^{3} \frac{4ig_{Wh_i H^\pm}\,\mathrm{Im}(g_{h_i \chi\chi})m_\chi}{m_{h_i}^2 - 4m_\chi^2 - im_{h_i}\Gamma_{h_i}} + \right.$$

11

$$+ \sum_{c=1}^{2} \frac{(g_{W\chi\tilde{\chi}_c^+}^R g_{H\chi\tilde{\chi}_c^+}^{R*} - g_{W\chi\tilde{\chi}_c^+}^L g_{H\chi\tilde{\chi}_c^+}^{L*})m_\chi + (g_{W\chi\tilde{\chi}_c^+}^L g_{H\chi\tilde{\chi}_c^+}^{R*} - g_{H\chi\tilde{\chi}_c^+}^R g_{H\chi\tilde{\chi}_c^+}^{L*})m_{\tilde{\chi}_c^+}}{m_{\tilde{\chi}_c^+}^2 + m_\chi^2 - (m_{H^\pm}^2 + m_W^2)/2 - im_{\tilde{\chi}_c^+}\Gamma_{\tilde{\chi}_c^+}} \Bigg|^2 , \quad (66)$$

$$\sigma_{h_i Z}v = \frac{\lambda_{h_i Z}^3 m_\chi^2}{16\pi m_Z^2} \left| \sum_{n=1}^{4} \frac{-2\,\mathrm{Re}(g_{Z\chi\chi}g_{h_i\chi_1\chi_n}^*)m_\chi + 2\,\mathrm{Re}(g_{Z\chi\chi}g_{h_i\chi_1\chi_n})m_{\chi_n}}{m_{\chi_n}^2 + m_\chi^2 - (m_{h_i}^2 + m_Z^2)/2 - im_{\chi_n}\Gamma_{\chi_n}} + \right.$$

$$\left. + \sum_{j=1}^{3} \frac{4ig_{Zh_j h_i}\,\mathrm{Im}(g_{h_j\chi\chi})m_\chi}{m_{h_j}^2 - 4m_\chi^2 - im_{h_j}\Gamma_{h_j}} - \frac{g_{h_i ZZ}\,\mathrm{Re}(g_{Z\chi\chi})}{m_Z^2} \right|^2 , \quad (67)$$

$$\sigma_{h_i h_j}v = \frac{\lambda_{hA}}{64\pi m_\chi^2} \left| \sum_{n=1}^{4} \frac{4\,\mathrm{Im}(g_{h_i\chi_1\chi_n}g_{h_j\chi_1\chi_n}^*)m_\chi m_{\chi_n} + (m_{h_i}^2 - m_{h_j}^2)\,\mathrm{Im}(g_{h_i\chi_1\chi_n}g_{h_j\chi_1\chi_n})}{m_{\chi_n}^2 + m_\chi^2 - (m_h^2 + m_Z^2)/2 - im_{\chi_n}\Gamma_{\chi_n}} + \right.$$

$$\left. + \sum_{k=1}^{3} \frac{2g_{h_i h_j h_k}\,\mathrm{Im}(g_{h_k\chi\chi})m_\chi}{m_{h_k}^2 - 4m_\chi^2 - im_{h_k}\Gamma_{h_k}} + \frac{ig_{Zh_i h_j}(m_i^2 - m_j^2)\,\mathrm{Re}(g_{Z\chi\chi})}{m_Z^2} \right|^2 . \quad (68)$$

N_f is 3 for quarks and 1 for leptons, $g_{h_i ff}$ and $g_{h_i\chi_m\chi_n}$ are given in eqs. (47–49), $g_{\tilde{f}\chi f}^L$ and $g_{\tilde{f}\chi f}^R$ are given in eqs. (8–11), and

$$g_{Wh_i H^\pm} = \frac{g}{2}\left[O'_{i1}\sin(\alpha - \beta) + O'_{i2}\cos(\alpha - \beta) + iO'_{i3}\right], \quad (69)$$

$$g_{Zh_i h_j} = \frac{ig}{2\cos\theta_W}\left[O'_{i1}\sin(\alpha - \beta) + O'_{i2}\cos(\alpha - \beta)\right]O'_{j3} - (i \leftrightarrow j), \quad (70)$$

$$g_{Zff}^A = \frac{gT_{3f}}{2\cos\theta_W}, \quad (71)$$

$$g_{W\chi\chi_c^+}^L = -\frac{gN_{14}V_{c2}^*}{\sqrt{2}} + gN_{12}V_{c1}^*, \quad (72)$$

$$g_{W\chi\chi_c^+}^R = +\frac{gN_{13}^* U_{c2}}{\sqrt{2}} + gN_{12}^* U_{c1}, \quad (73)$$

$$g_{Z\chi_m\chi_n} = \frac{g}{2\cos\theta_W}\left(N_{m4}N_{n4}^* - N_{m3}N_{n3}^*\right). \quad (74)$$

Here V and U are the chargino mixing matrices.

For real μ and real gaugino masses, as we assume here, the terms containing $\mathrm{Im}(g_{W\chi\tilde{\chi}_c^+}^L g_{W\chi\tilde{\chi}_c^+}^{R*})$ and $\mathrm{Im}(g_{Z\chi\chi_n}^2)$ in eqs. (64–65) vanish.

Notice that in the annihilation into fermion pairs, in the first terms under absolute values in eq. (63) (see fig. 1(a)), there can be contributions from all Higgs bosons h_i for which the imaginary part of $g_{h_i\chi\chi}$ is non-zero. Examining eq. (49) for the couplings, recalling that the matrix elements O'_{ij} are real and that for real μ and real gaugino masses $N_{1i}N_{1j}$ are also real, we see that the h_i contributes when O'_{i3} is non-zero. In the CP-conserving case, this happens only for $i = 3$, i.e. for the A boson, while with CP violation this occurs also for $i = 1$ and $i = 2$. The annihilation into $f\bar{f}$ then proceeds through exchange of all Higgs bosons, raising the possibility of resonant annihilation when $2m_\chi$ is approximately equal to the mass of any Higgs boson. This phenomenon is peculiar to CP violation. An example is given in fig. 9 below.

VIII. RESULTS

A. Results for the elastic scattering cross section

In Figure 2 we show the neutralino–proton elastic scattering cross section as a function of neutralino mass for the $\sim 10^6$ values in SUSY parameter space that we consider. There is no CP violation in the lower panel (Im $A = 0$), while CP violation is allowed in the upper panel. Also shown are the present experimental bounds from the DAMA [36] and CDMS [37] collaborations as well as the future reach of the CDMS (Soudan) [37], CRESST [38] and GENIUS [39] experiments. In the upper panel, it is the maximally enhanced cross section (as a function of arg(A)) that is plotted. The red (dark) points refer to those values of parameter space which have the maximum value of the cross section for nonzero Im(A) and which are experimentally excluded at zero Im(A). The blue (grey) region refers to those values of parameter space which are enhanced when CP violation is included and which are allowed also at zero Im(A). The green (light grey) empty squares refer to those values of parameter space which have no enhancement when CP violation is included. From the existence of the red points we conclude that there are indeed points in SUSY parameter space which are ruled out experimentally when CP is conserved but are allowed when CP is violated.

By comparing corresponding points in the upper and lower panels of figure 2, we notice that there can be enhancement or suppression of the cross section when we allow for CP violation. There are two types of enhancement: one in which the model without CP violation is allowed and another in which it is experimentally ruled out. In the first case, it is possible to define a ratio between enhanced and unenhanced cross sections, $R_{\max} = \sigma^{\max}/\sigma^0_{\max}$. in the second case, when both $\sigma(0)$ and $\sigma(\pi)$ are excluded, it is not possible to define the previous ratio. Here $\sigma^{\max}$ is the maximally enhanced cross section as one goes through the phase of A, and $\sigma^0_{\max} = \max[\sigma(0), \sigma(\pi)]$ is the larger of the unenhanced CP conserving cross sections. We plot $R^{\max}$ in figure 3 as a function of $\sigma^0_{\max}$. In those models in parameter space that we have considered, we notice that the enhancement due to CP violation is at most a factor of two.

In figure 3, we have also plotted the ratio $R_{\min} = \sigma^{\min}/\sigma^0_{\min}$, which is a measure of the maximal suppression of the neutralino–proton cross section when CP violation is included. Here $\sigma^{\min}$ is the maximally suppressed cross section as one goes through the phase of A, and $\sigma^0_{\min} = \min[\sigma(0), \sigma(\pi)]$ is the smaller of the unenhanced CP conserving cross sections. We see that significant suppression of the scattering cross section, as low as 10^{-7}, is possible.

In figure 4, we show the dependence of these enhancement and suppression factors $R_{\max}$ and $R_{\min}$ on the phase ϕ_A of A. The points are plotted at those values of ϕ_A at which the maximum or minimum of the scattering cross section occurs.

B. Results for the annihilation cross section

We also have obtained values for the neutralino annihilation cross section σv for the case of CP violation through the phase of A. In figure 5 we show the maximum value of σv obtained as we vary ϕ_A as a function of neutralino mass. As in the analogous Figure 2 for

the scattering cross section, the upper panel includes CP violation while the lower one does not. The distinction between red (dark), blue (grey), and green (light grey) points is as in Figure 2.

Figure 6 shows the enhancement of the annihilation cross section via the ratio $R_{\mathrm{max}}^{\mathrm{ann}} = (\sigma v)^{\mathrm{max}}/(\sigma v)_{\mathrm{max}}^0$. We see that the annihilation cross section can be significantly enhanced for CP violation with $\mathrm{Im}(A) \neq 0$, by as much as a factor of 10^6. In all models for which we find an enhancement in the annihilation cross section of at least 10^3, the enhancement is due to an s-channel resonance with the exchange of one of the Higgs bosons h_1, h_2 or h_3. See fig. 9 for an example.

A similar ratio can be constructed for $R_{\mathrm{min}}^{\mathrm{ann}}$ to show that the suppression due to CP violation can be roughly a factor of 50. The dependence of these enhancement and suppression factors $R_{\mathrm{max}}^{\mathrm{ann}}$ and $R_{\mathrm{min}}^{\mathrm{ann}}$ on ϕ_A are plotted in figure 7.

C. Phase dependence of the results

In the four panels in each of the fig. 8–11 we display the behavior of the scattering cross section $\sigma_{\chi p}$, the annihilation cross section σv, the branching ratio $\mathrm{BR}(b \to s\gamma)$, and the lightest Higgs boson mass m_{h_1} as a function of the phase ϕ_A of A. In the third and fourth panels we hatch the regions currently ruled out by accelerator experiments. In all four panels we denote the part of the curves that is experimentally allowed by thickened solid lines, and the part that is experimentally ruled out (as seen e.g. in the third and fourth panels) by thinner solid lines.

For the models shown in figs. 8–11, we give the values of the input parameters and of the neutralino mass and composition (gaugino fraction $|N_{11}|^2 + |N_{12}|^2$) in table 2.

In the case plotted in fig. 8, the possible phases are bound by the limit on the $b \to s\gamma$ branching ratio. In the allowed regions, the scattering cross section at CP-violating phases is suppressed, while the annihilation cross section is enhanced. The latter takes its maximum allowed value when the $b \to s\gamma$ limit is reached.

Figure 9 presents another case in which the phase of A is bounded by the $b \to s\gamma$ branching ratio. Here the scattering cross section is enhanced by only 2%, while the annihilation cross section is enhanced by a factor of $\simeq 222$ at $\phi_A \simeq 0.129\pi$. This is due to a resonant annihilation of the neutralinos through s-channel exchange of the h_1 Higgs boson (fig. 1(a)), which occurs when $2m_\chi = m_{h_1}$ (see the lowest panel). Notice that in the CP conserving case, the s-channel exchange of the CP-even h_1 boson vanishes at $v = 0$ because for real $\chi\chi h_1$ couplings the amplitude is proportional to $\overline{\chi}\chi$ which is zero at $v = 0$. In presence of CP violation, the $\chi\chi h_1$ couplings are in general complex, and the amplitude contains a contribution from $\overline{\chi}\gamma_5\chi$ which does not vanish at $v = 0$. So the h_1 resonant annihilation seen in fig. 9 is only possible when CP is violated.

Figure 10 shows a case which is experimentally allowed for all values of the phase ϕ_A. The maximum of the scattering cross section takes place at the CP-conserving value $\phi_A = \pi$ and the minimum at $\phi_A = 0$. The annihilation cross section on the other hand is enhanced by CP violation, as can be seen in the second panel. Notice that its maximum occurs at $\phi_A = 0.41\pi$, which is not the point of maximal CP violation $\phi_A = \pi/2$.

Finally fig. 11 displays an example in which both CP conserving cases are experimentally excluded while some CP violating cases are allowed. This is one of the red (dark) points in fig. 5. The $\phi_A = 0$ case is ruled out by the bounds on both $\mathrm{BR}(b \to s\gamma)$ and the Higgs mass, the $\phi_A = \pi$ case by only the bound on the Higgs mass. Notice that the scattering cross section is of the order of 10^{-6} pb, in the region probed by the direct detection experiments. The annihilation cross section peaks at $\phi_A = 3\pi/4$; notice that again this value is not the point of maximal CP violation $\phi_A = \pi/2$.

IX. CONCLUSIONS

We have examined the effect of CP violation on the neutralino annihilation and scattering cross sections, which are of importance in calculations of the neutralino relic density and of the predicted rates for direct and indirect searches of neutralino dark matter. Specifically we have considered the case in which the only CP violating phase in addition to the standard model CKM phase is in the complex soft trilinear scalar couplings A of the third generation. This phase affects the squark masses and through radiative corrections generates a mixing between CP-even and CP-odd Higgs bosons. This mixing modifies the neutralino annihilation and scattering cross sections in the kinematic regimes relevant for dark matter detection. Exploring $\sim 10^6$ points in supersymmetric parameter space with a non-zero phase of A, we have found that: (1) the scattering cross section is generally suppressed, even by 7 orders of magnitude in special cases; (2) the annihilation cross section can be enhanced by factors of 10^6 as resonant neutralino annihilation through a Higgs boson becomes possible at CP-violating values of the phase of A. We have also found cases which are experimentally excluded when CP conservation is imposed but are allowed when CP conservation is violated. Some of these cases have neutralino masses and cross sections in the region probed by current dark matter searches.

ACKNOWLEDGMENTS

REFERENCES

[1] M.W. Goodman and E. Witten, Phys. Rev. D31, 3059 (1985).

[2] J. Silk, K.A. Olive and M. Srednicki, Phys. Rev. Lett. 55, 257 (1986); K. Freese, Phys. Lett. B167, 295 (1986); L.M. Krauss, M. Srednicki, and F. Wilczek, Phys. Rev. D33, 2079 (1986).

[3] J.E. Gunn, B.W. Lee, I. Lerche, D.N. Schramm, and G. Steigman, Ap. J. 223, 1015 (1978); F.W. Stecker, Ap. J. 223, 1032 (1978).

[4] T. Falk, A. Ferstl, and K.A. Olive, Phys. Rev. D59, 055009 (1999).

[5] A. Pilaftsis, Phys. Lett. B435, 88 (1998).

[6] H.E. Haber, in Review of Particle Properties, C. Caso et al. (Particle Data Group), Europ. Phys. J. C3 (1998) 1.

[7] S. Dimopoulos and D. Sutter, Nucl. Phys. **B465**, 23 (1995).

[8] L. Bergström and P. Gondolo, Astropart. Phys. **5**, 183 (1996).

[9] J. Edsjö and P. Gondolo, Phys. Rev. **D56**, 1879 (1997).

[10] L. Bergström, P. Ullio, and J. H. Buckley, Astropart. Phys. **9**, 137 (1998).

[11] P. Gondolo et al., 1999.

[12] J. Ellis, G. Ridolfi, and F. Zwirner, Phys. Lett. B262 (1991) 477.

[13] A. Blondel, F. Gianotti, Y. Gao and P. Gay (ALEPH Collab.), in "High Energy Physics 99," Tampere, Finland, July 1999 (ALEPH 99-053, CONF 99-029,URL: http://alephwww.cern.ch/ALPUB/conf/conf.html).

[14] S. Bertolini, F. Borzumati, A. Masiero, and G. Ridolfi, Nucl. Phys. B353, 591 (1991).

[15] D. Chang, W.-Y. Keung, A. Pilaftsis, Phys. Rev. Lett. 82, 900 (1999).

[16] A. Manohar and H. Georgi, Nucl. Phys. B234, 189 (1984).

[17] T. Ibrahim and P. Nath, Phys. Rev. D57, 478 (1998).

[18] E.D. Commins, S.B. Ross, D. DeMille, and B.C. Regan, Phys. Rev. A50, 2960 (1994).

[19] I.S. Altarev et al., Phys. Atomic Nuclei 59, 1152 (1996).

[20] C. Caso et al. (Particle Data Group), Europ. Phys. J. C3, 1 (1998), and 1999 partial update for edition 2000 (URL: http://pdg.lbl.gov)

[21] G. Abbiendi et al. (OPAL Collab.), Europ. Phys. J. C7, 407 (1999).

[22] J. Carr et al. (ALEPH Collab.), talk to LEPC, 31 March 1998 (URL: http://alephwww.cern.ch/ALPUB/seminar/carrlepc98/index.html).

[23] M. Acciarri et al. (L3 Collab.), Phys. Lett. B377, 289 (1996).

[24] D. Decamp et al. (ALEPH Collab.), Phys. Rep. 216, 253 (1992).

[25] K. Hidaka, Phys. Rev. D44, 927 (1991).

[26] M. Acciarri et al. (L3 Collab.), Phys. Lett. B350, 109 (1995).

[27] D. Buskulic et al. (ALEPH Collab.), Zeitschrift für Physik C72, 549 (1996).

[28] M. Acciarri et al. (L3 Collab.), Europ. Phys. J. C4, 207 (1998).

[29] G. Abbiendi et al. (OPAL Collab.), Europ. Phys. J. C8, 255 (1999).

[30] S. Abachi et al. (D0 Collab.), Phys. Rev. Lett. 75, 618 (1995).

[31] F. Abe et al. (CDF Collab.), Phys. Rev. D56, R1357 (1997).

[32] F. Abe et al. (CDF Collab.), Phys. Rev. Lett. 69, 3439 (1992).

[33] F. Abe et al. (CDF Collab.), Phys. Rev. Lett. 76, 2006 (1996).

[34] R. Barate et al. (ALEPH Collab.), Phys. Lett. B433, 176 (1998).

[35] J. Gasser, H. Leutwyler, and M.E. Sainio, Phys. Lett. B253, 252 (1991); M. Drees and M. Nojiri, Phys. Ref. D48, 3483 (1993).

[36] R. Bernabei et al. (DAMA Collab.), Phys. Lett. B389, 757 (1997).

[37] R. Schnee (for the CDMS Collab.), talk presented at "Inner Space/Outer Space II," Fermilab, May 1999.

[38] M. Bravin et al. (CRESST Collab.), hep-ex/9904005.

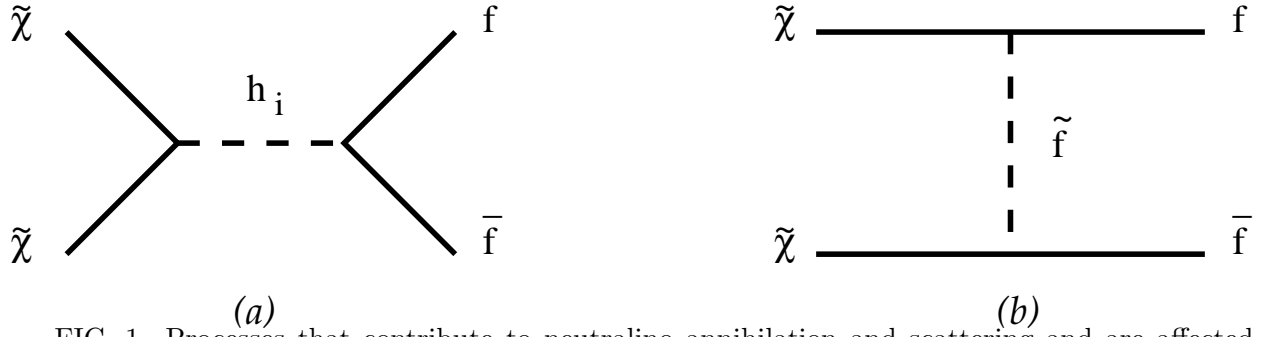[39] L. Baudis et al. (GENIUS Collab.), Phys. Rep. 307, 301 (1998).

(a)   *(b)*

FIG. 1. Processes that contribute to neutralino annihilation and scattering and are affected by the CP violating phase of A. For annihilation: (a) s-channel diagrams via the three neutral Higgs bosons h_1, h_2, and h_3 into final state fermions f, and (b) t-channel diagrams via intermediate squarks $\tilde{f}$ into final state fermions. For scattering: crossed diagrams.

Bound	Ref.
$\Gamma_Z^{\mathrm{inv}} < 502.4\mathrm{MeV}$	[20]
$m_{H^\pm} > 59.5\mathrm{GeV}$	[21]
$m_{h_i} > 82.5\mathrm{GeV}$	[13]
$m_{\tilde{\chi}_1^+} > 91\mathrm{GeV}$ if $m_{\tilde{\chi}_1^0} - m_{\tilde{\chi}_2^+} > 4\mathrm{GeV}$	[22]
$m_{\tilde{\chi}_1^+} > 64\mathrm{GeV}$ if $m_{\tilde{\chi}_1^0} > 43\mathrm{GeV}$ and $m_{\tilde{\chi}_2^+} > m_{\tilde{\chi}_2^0}$	[23]
$m_{\tilde{\chi}_1^+} > 47\mathrm{GeV}$ if $m_{\tilde{\chi}_1^0} > 41\mathrm{GeV}$	[24]
$m_{\tilde{\chi}_2^+} > 99\mathrm{GeV}$	[25]
$m_{\tilde{\chi}_1^0} > 23\mathrm{GeV}$ if $\tan\beta > 3$	[26]
$m_{\tilde{\chi}_1^0} > 20\mathrm{GeV}$ if $\tan\beta > 2$	[26]
$m_{\tilde{\chi}_1^0} > 12.8\mathrm{GeV}$ if $m_{\tilde{\nu}} < 200\mathrm{GeV}$	[27]
$m_{\tilde{\chi}_1^0} > 10.9\mathrm{GeV}$	[28]
$m_{\tilde{\chi}_2^0} > 44\mathrm{GeV}$	[29]
$m_{\tilde{\chi}_3^0} > 102\mathrm{GeV}$	[29]
$m_{\tilde{\chi}_4^0} > 127\mathrm{GeV}$	[26]
$m_{\tilde{g}} > 212\mathrm{GeV}$ if $m_{\tilde{q}_k} < m_{\tilde{g}}$	[30]
$m_{\tilde{g}} > 162\mathrm{GeV}$	[31]
$m_{\tilde{q}_k} > 90\mathrm{GeV}$ if $m_{\tilde{g}} < 410\mathrm{GeV}$	[32]
$m_{\tilde{q}_k} > 176\mathrm{GeV}$ if $m_{\tilde{g}} < 300\mathrm{GeV}$	[30]
$m_{\tilde{q}_k} > 224\mathrm{GeV}$ if $m_{\tilde{g}} > m_{\tilde{g}}$	[33]
$m_{\tilde{e}} > 78\mathrm{GeV}$ if $m_{\tilde{\chi}_1^0} < 73\mathrm{GeV}$	[34]
$m_{\tilde{\mu}} > 71\mathrm{GeV}$ if $m_{\tilde{\chi}_1^0} < 66\mathrm{GeV}$	[34]
$m_{\tilde{\tau}} > 65\mathrm{GeV}$ if $m_{\tilde{\chi}_1^0} < 55\mathrm{GeV}$	[34]
$m_{\tilde{\nu}} > 44.4\mathrm{GeV}$	[20]
$1 \times 10^{-4} < \mathrm{BR}(b \to s\gamma) < 4 \times 10^{-4}$	[20]
$|d_e| < 0.4 \times 10^{-26} e\mathrm{cm}$	[18]
$|d_n| < 1.79 \times 10^{-25} e\mathrm{cm}$	[19]

TABLE I. Experimental bounds we use in this paper. We do not include cosmological bounds nor bounds from dark matter searches.

	JEsp4_001509	JE27_004174	JE28_002656	JEsp4_002809
	Fig. 8	Fig. 9	Fig. 10	Fig. 11
μ [GeV]	-331.433	-271.973	-234.128	958.213
M_2 [GeV]	390.064	106.141	338.688	-153.256
m_A [GeV]	84.2527	168.935	325.691	106.804
$\tan\beta$	31.6126	4.37629	1.80096	48.4750
$\widetilde{M}$ [GeV]	1085.05	494.379	1856.43	890.647
$A/\widetilde{M}$	2.71920	0.661158	1.88819	-2.05440
m_χ [GeV]	191.46	54.95	172.4	77.04
$|N_{11}|^2 + |N_{12}|^2$	0.9459	0.9806	0.9571	0.99786

TABLE II. Model parameters and neutralino mass and composition (gaugino fraction) for the examples in figs. 8–11.
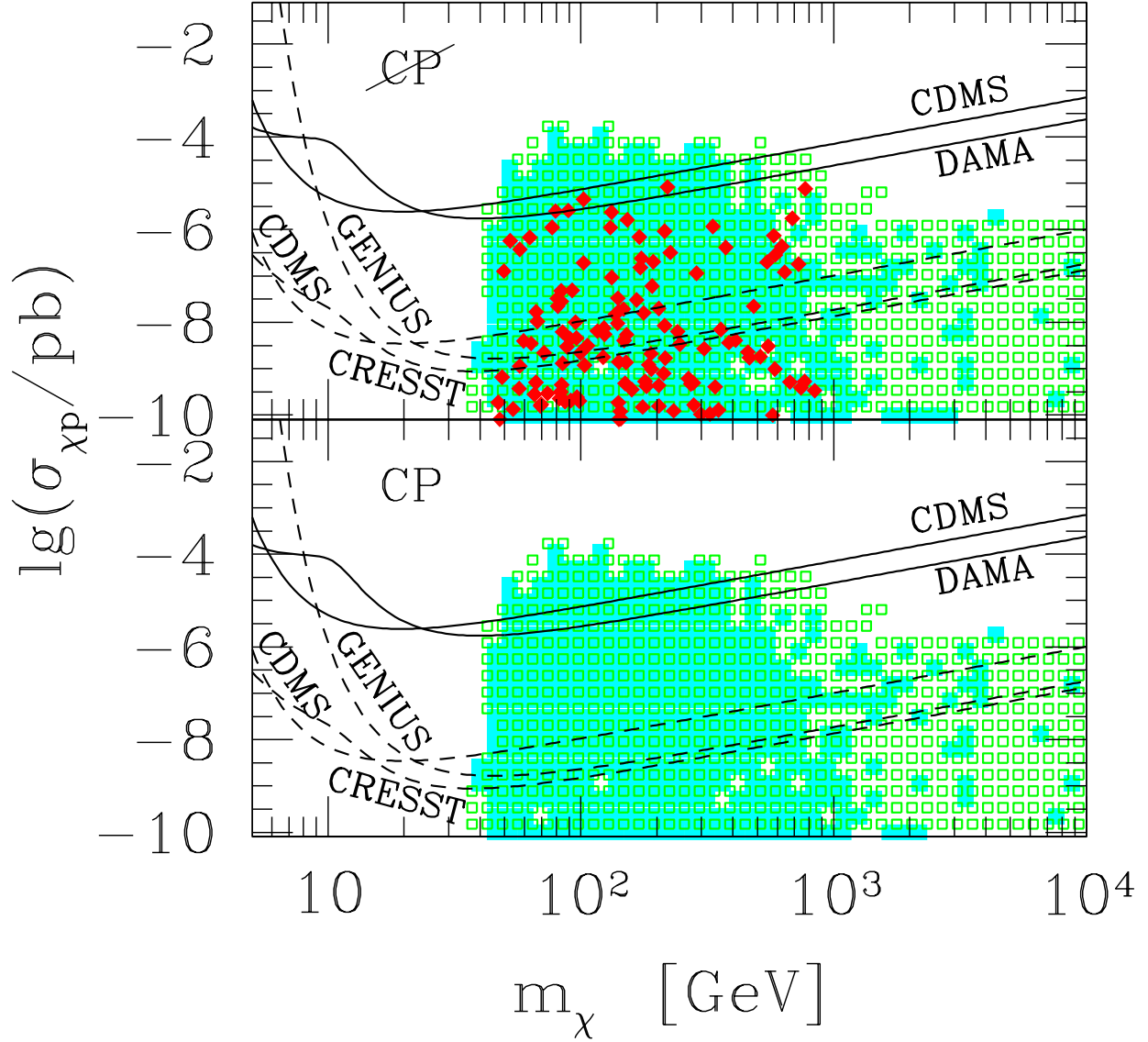
FIG. 2. Neutralino elastic scattering cross section (in pb) as a function of neutralino mass (in GeV) for $\sim 10^6$ values in SUSY parameter space. The upper panel is for the case of CP violation via $\mathrm{Im}(A) \neq 0$ while the lower panel is for the case of no CP violation. In the upper panel, it is the maximally enhanced cross section (as a function of $\arg(A)$) that is plotted. The red (dark) points refer to those values of parameter space which have the maximum value of the cross section for nonzero $\mathrm{Im}(A)$ and which are experimentally excluded at zero $\mathrm{Im}(A)$. The blue (grey) region refer to those values of parameter space which are enhanced when CP violation is included and which are allowed also at zero $\mathrm{Im}(A)$. The green (light grey) empty squares refer to those values of parameter space which have no enhancement when CP violation is included. The solid lines indicate the current experimental bounds placed by DAMA and CDMS; the dashed lines indicate the future reach of the CDMS (Soudan), GENIUS, and CRESST proposals.

21
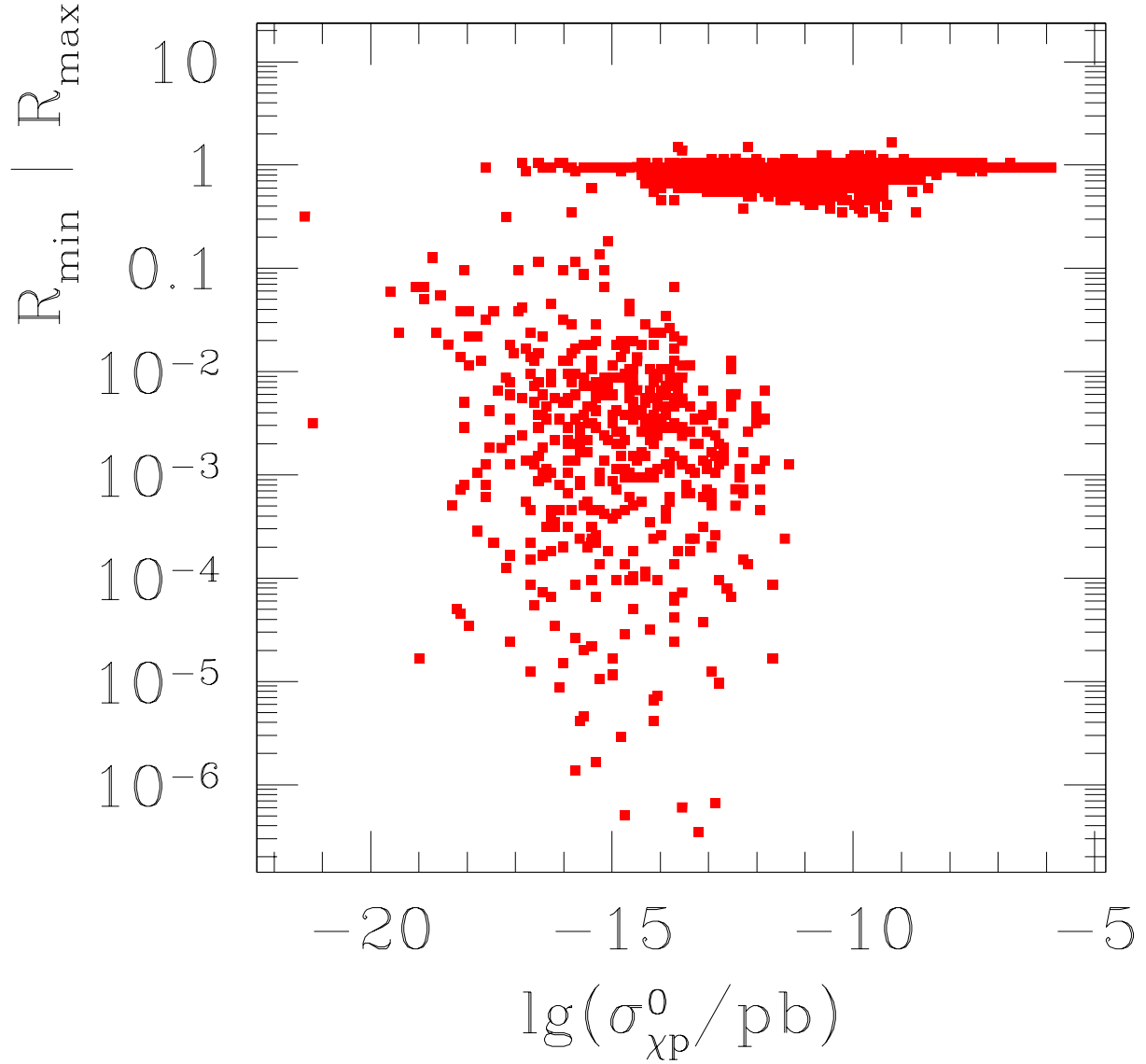
FIG. 3. Enhancement and suppression of elastic scattering cross section for the case of CP violating $\arg(A)$. The plot shows the ratio $R_{\mathrm{max}} = \sigma^{\mathrm{max}}/\sigma^0_{\mathrm{max}}$ as a function of the unenhanced scattering cross section $\sigma^0_{\mathrm{max}} = \max[\sigma(0), \sigma(\pi)]$. Here σ^{max} is the enhanced scattering cross section and the superscript max indicates the maximal enhancement as one goes through the phase of A. The denominator of the ratio R_{max} chooses the larger value of the scattering cross section without CP violation, i.e., for phase = 0 or phase = π. Similarly, the ratio $R_{\mathrm{min}} = \sigma^{\mathrm{min}}/\sigma^0_{\mathrm{min}}$ is plotted; this time the denominator chooses the smaller value of the scattering cross section without CP violation, $\sigma^0_{\mathrm{min}} = \min[\sigma(0), \sigma(\pi)]$.

22
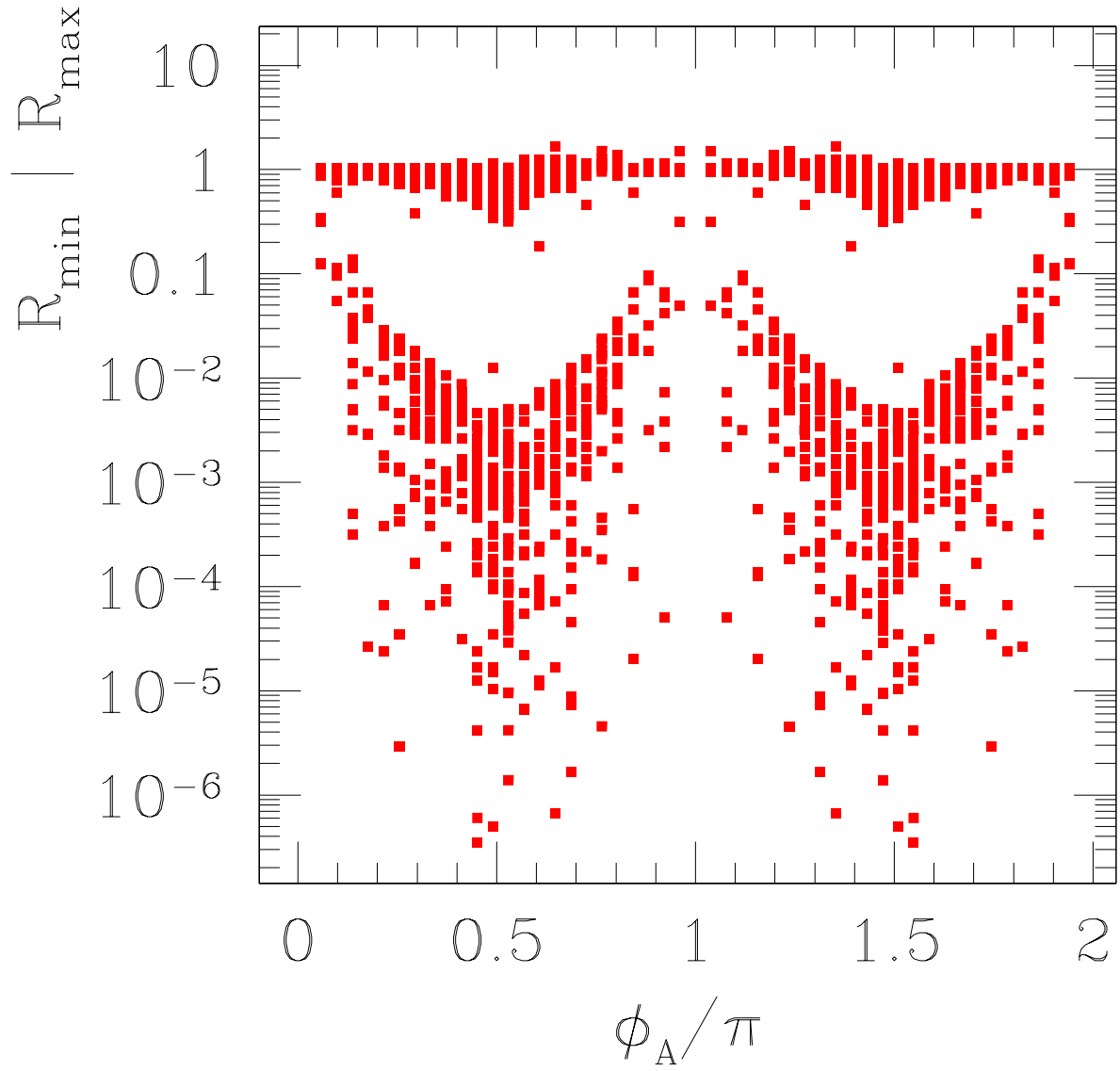
FIG. 4. The enhancement/suppression factors $R_{\max}$ and $R_{\min}$ defined in the caption of figure 3 as a function of the values ϕ_A of the phase of A where the maximum/minimum occur.
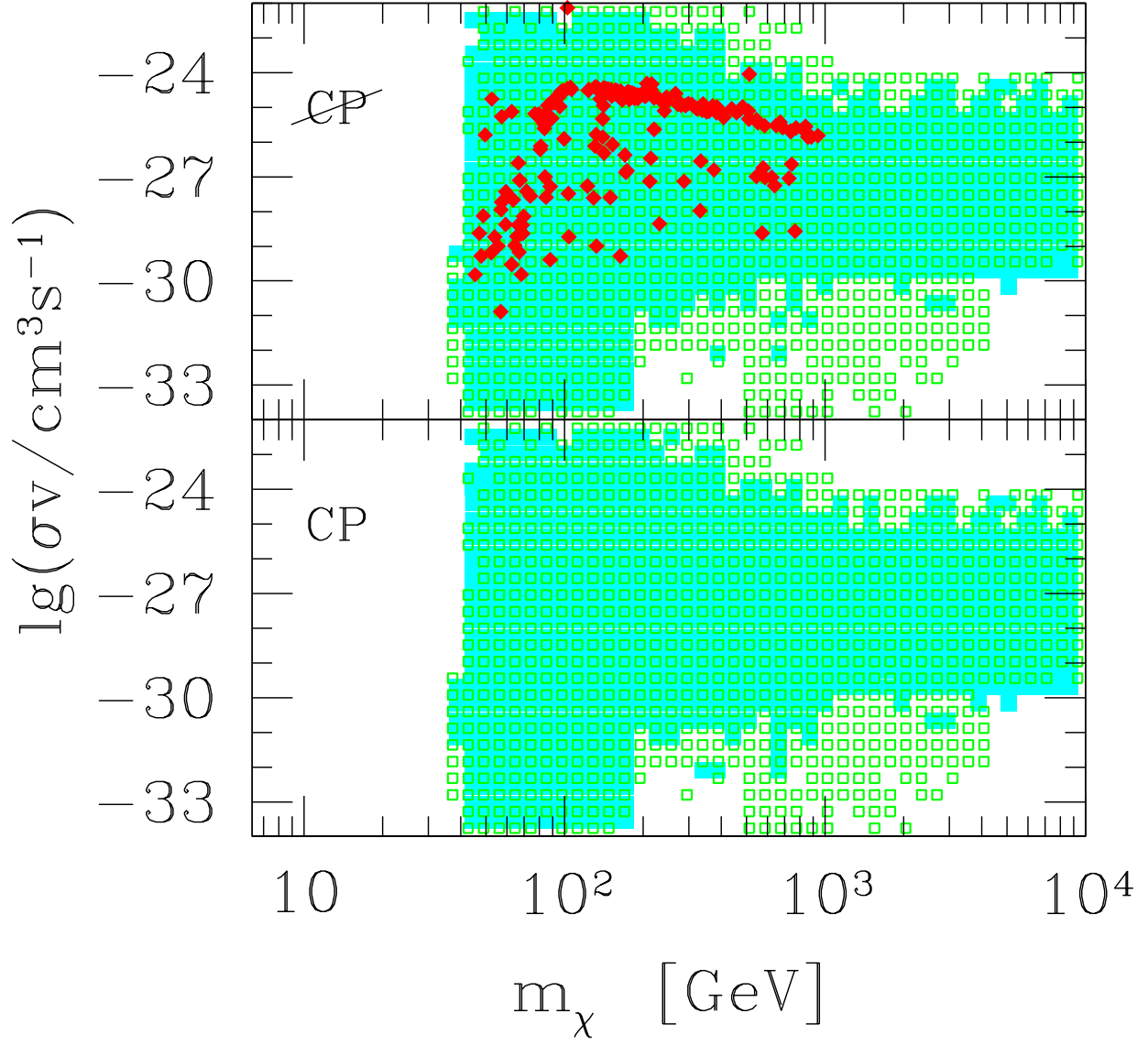
FIG. 5. Same as fig. 2 but for the neutralino annihilation cross section times relative velocity σv (in cm^3/s at $v = 0$) as a function of neutralino mass (in GeV) for $\sim 10^6$ values in SUSY parameter space.
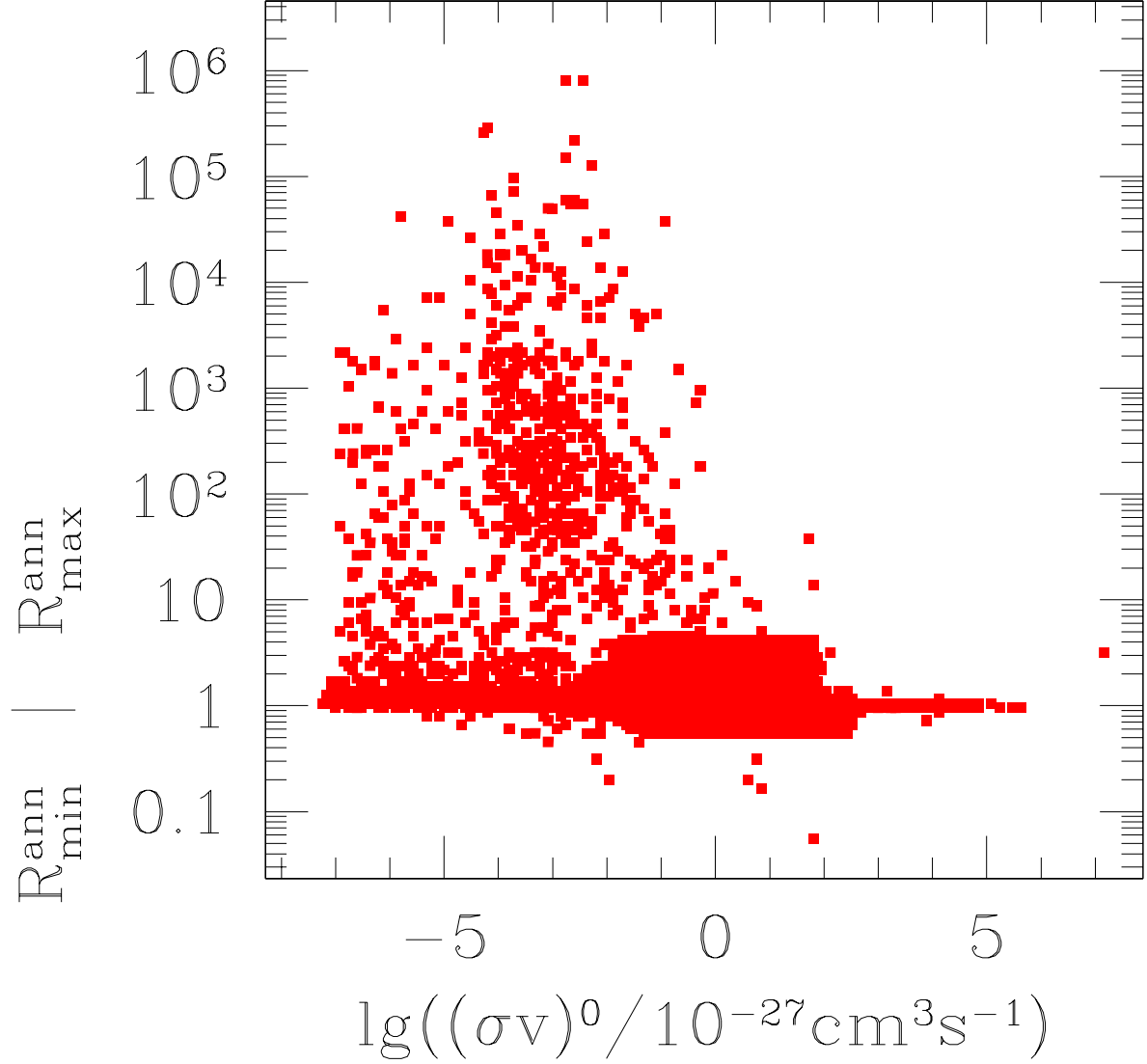
FIG. 6. Enhancement and suppression of neutralino annihilation cross section for the case of CP violating $\arg(A)$. The plot shows the ratio $R^{\text{ann}}_{\text{max}} = (\sigma v)^{\text{max}}/(\sigma v)^{0}_{\text{max}}$ as a function of the unenhanced annihilation cross section $(\sigma v)^{0}_{\text{max}} = \max[\sigma v(0), \sigma v(\pi)]$. Here $(\sigma v)^{\text{max}}$ is the enhanced scattering cross section and the superscript max indicates the maximal enhancement as one goes through the phase of A. The denominator of the ratio $R^{\text{ann}}_{\text{max}}$ chooses the larger value of the scattering cross section without CP violation, i.e., for phase $= 0$ or phase $= \pi$. Similarly, the ratio $R^{\text{ann}}_{\text{min}} = (\sigma v)^{\text{min}}/(\sigma v)^{0}_{\text{min}}$ is plotted. Here $(\sigma v)^{0}_{\text{min}} = \min[\sigma v(0), \sigma v(\pi)]$.
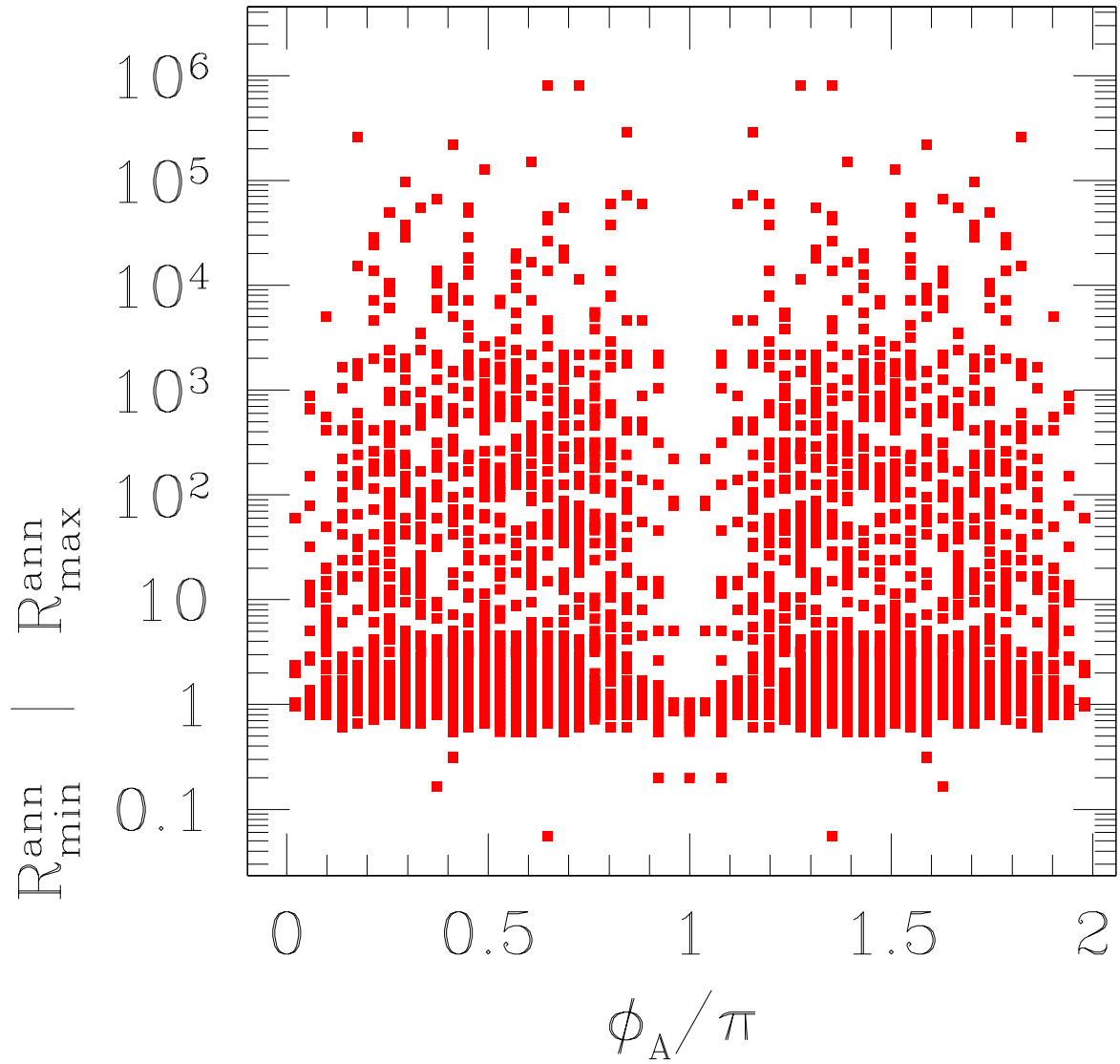
FIG. 7. The enhancement/suppression factors $R_{\text{max}}^{\text{ann}}$ and $R_{\text{min}}^{\text{ann}}$ defined in the caption of figure 6 as a function of the values ϕ_A of the phase of A where the maximum/minimum occur.
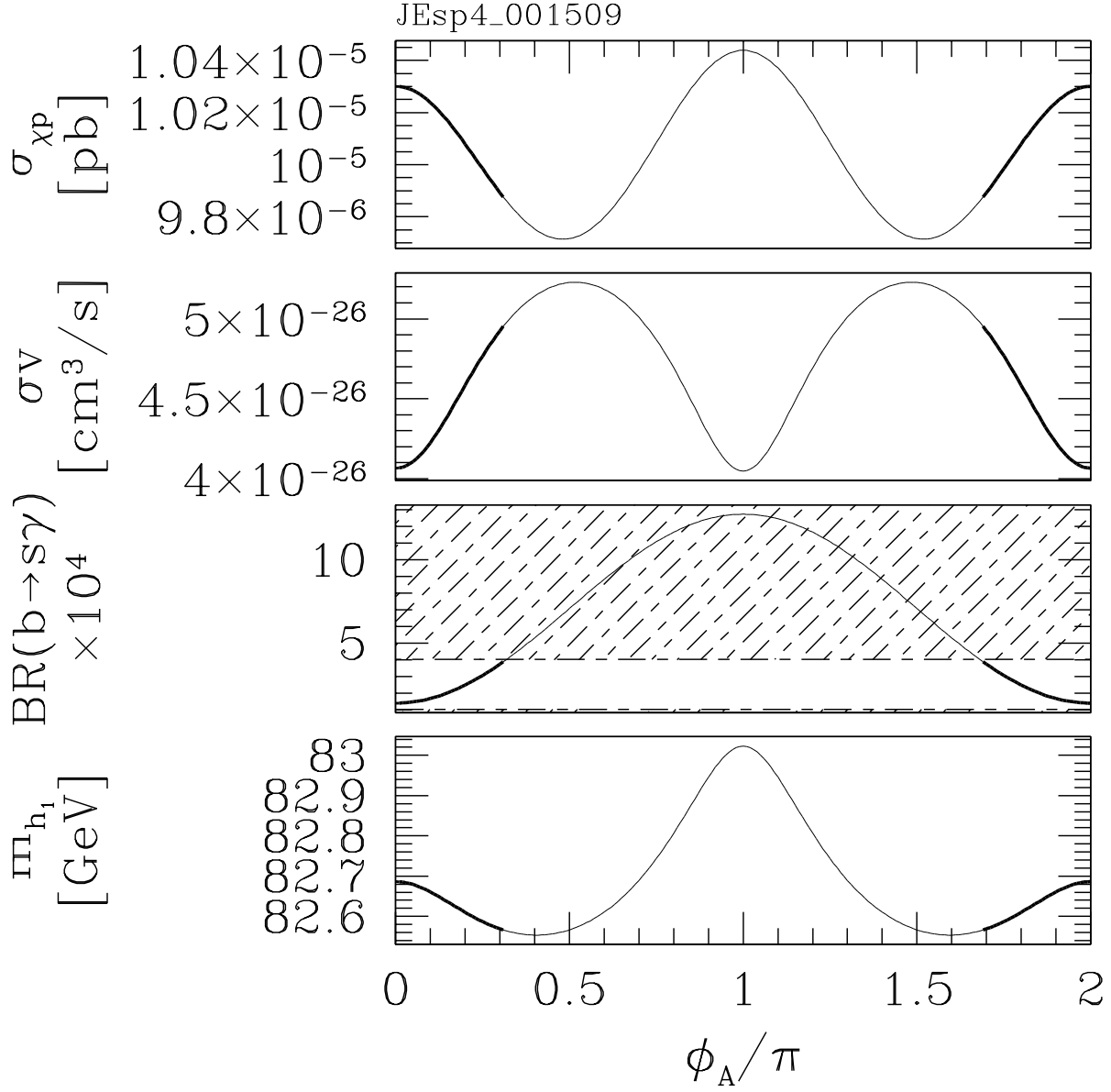
FIG. 8. The four panels from top to bottom display the following: the scattering cross section $\sigma_{\chi p}$ in pb, the annihilation cross section σv in cm^3/s, the branching ratio $BR(b \to s\gamma) \times 10^4$, and the lightest Higgs boson mass m_{h_1} in GeV as a function of the phase ϕ_A of A. CP conserving phases are $\phi_A = 0, \pi$ while all other values are CP violating. In the third and fourth panels we hatch the regions currently ruled out by accelerator experiments. In all four panels we denote the part of the curves that is experimentally allowed by thickened solid lines, and the part that is experimentally ruled out by thinner solid lines. In this figure, the possible phases are bound by the limit on the $b \to s\gamma$ branching ratio. In the allowed regions, the scattering cross section at CP-violating phases is suppressed, while the annihilation cross section is enhanced. The latter takes its maximum allowed value when the $b \to s\gamma$ limit is reached.
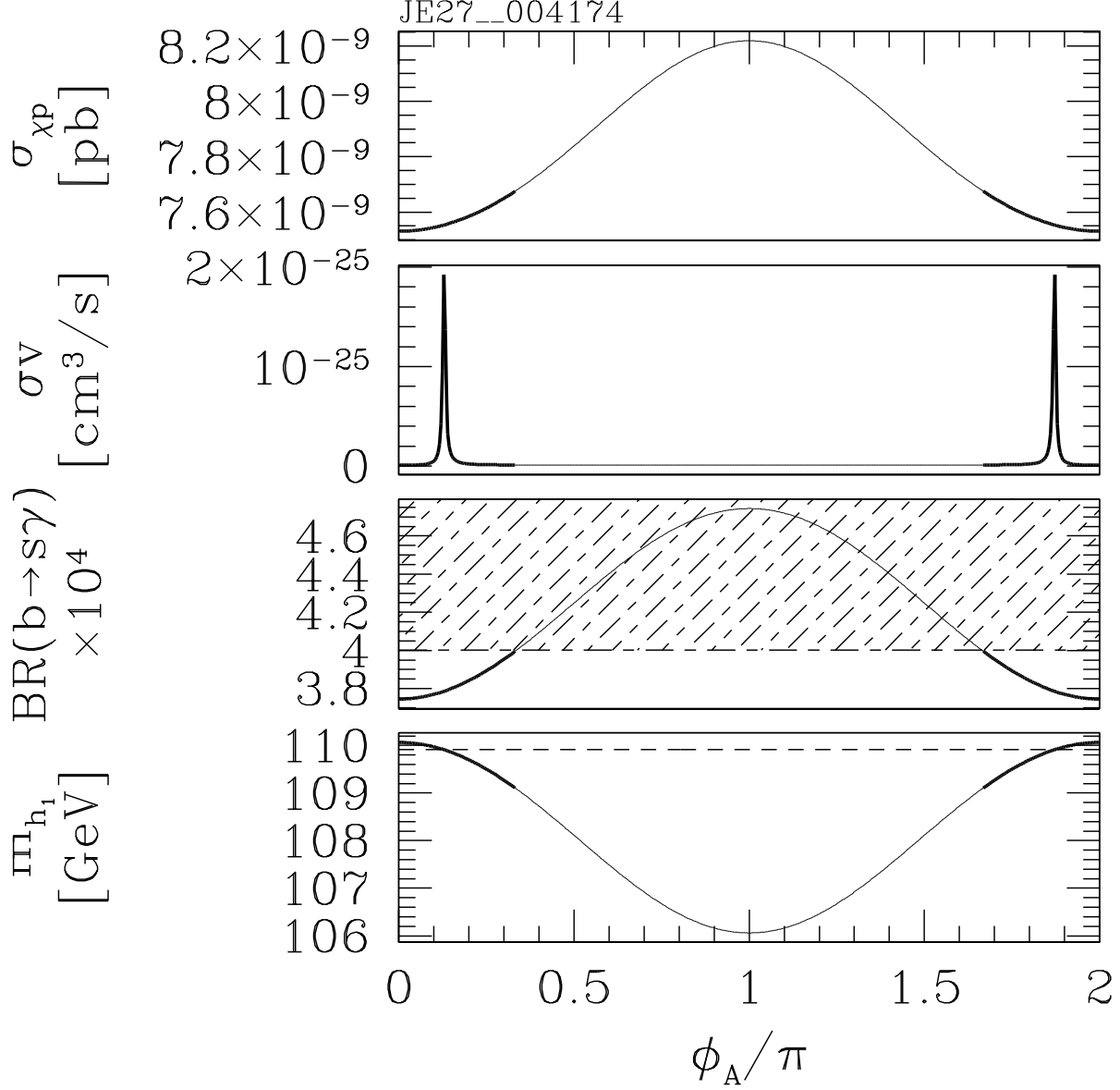
FIG. 9. Same notation as fig. 8. The phase of A is bounded by the $b \to s\gamma$ branching ratio, the scattering cross section is enhanced by only 2%, and the annihilation cross section is enhanced by a factor of $\simeq 222$ at $\phi_A \simeq 0.129\pi$, where the annihilation proceeds through the h_1 resonance at $2m_\chi = m_{h_1}$ (see bottom panel).
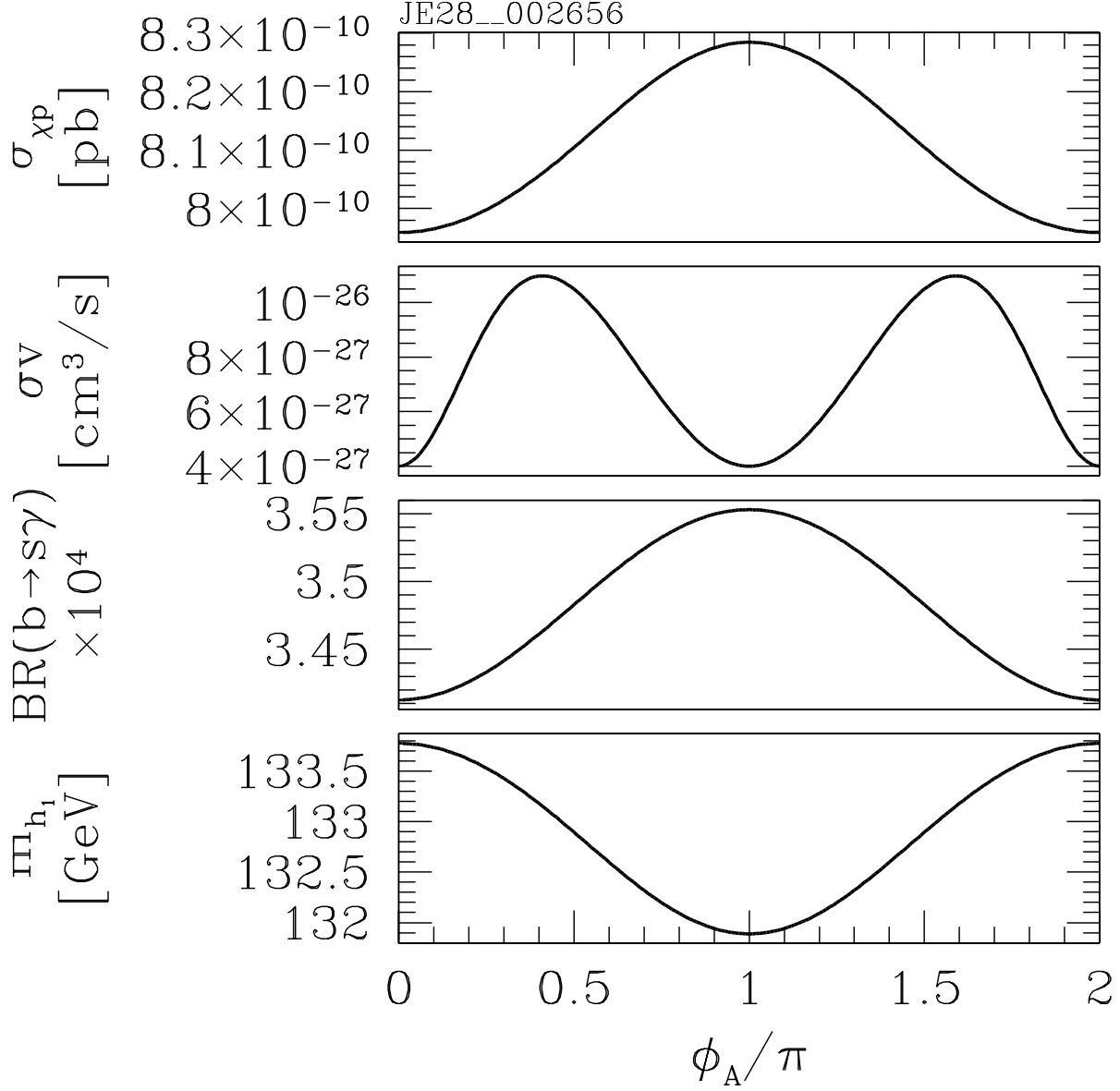
FIG. 10. *"The Duck."* Same notation as fig. 8. This case is experimentally allowed for all values of the phase ϕ_A. The maximum of the scattering cross section takes place at the CP-conserving value $\phi_A = \pi$ and the minimum at $\phi_A = 0$. The annihilation cross section is enhanced by CP violation, as can be seen in the second panel.
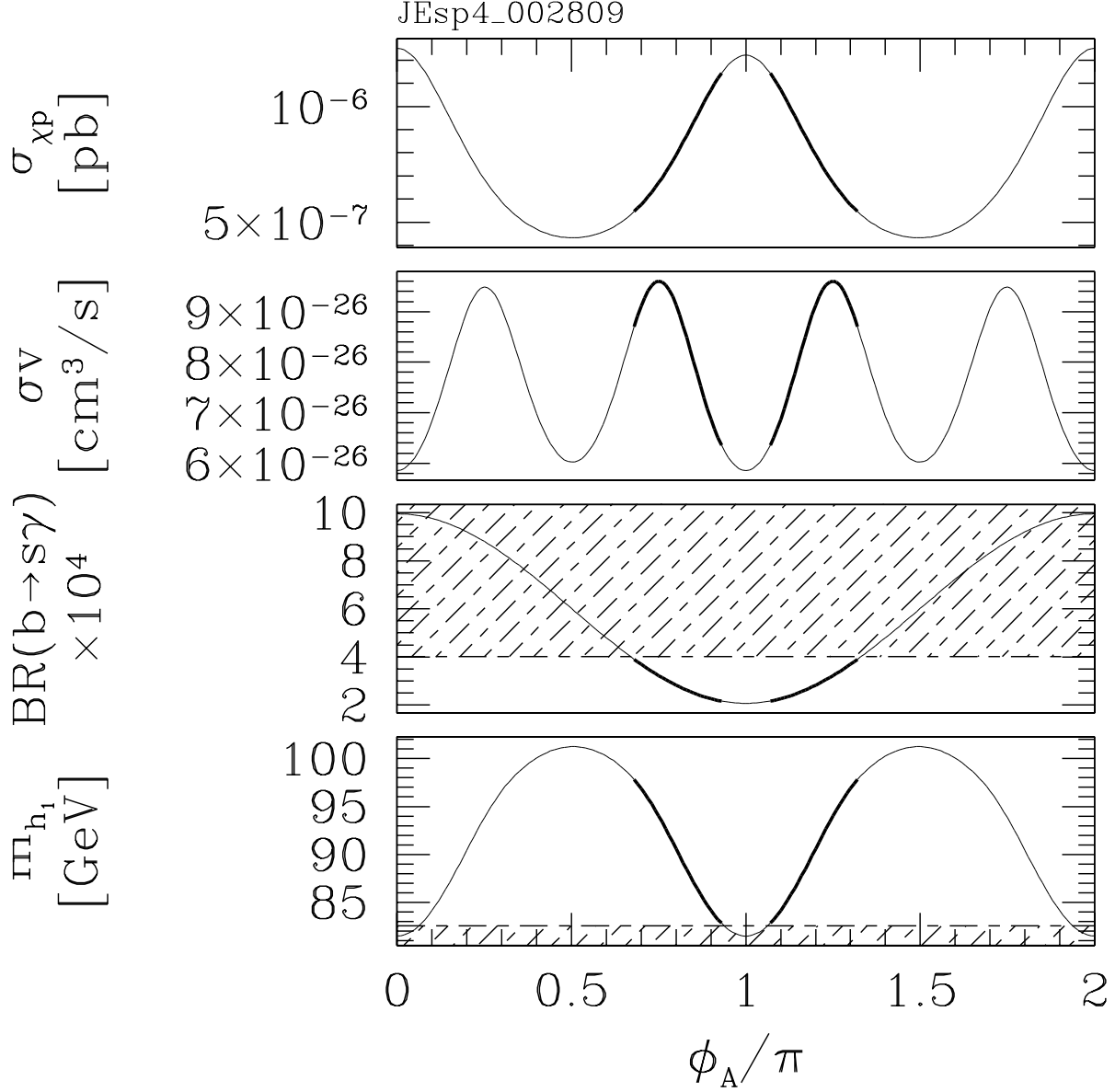
FIG. 11. Same notation as fig. 8. Here, both CP conserving cases are experimentally excluded while some CP violating cases are allowed. This is one of the red (dark) points in fig. 5. The scattering cross section is of the order of 10^{-6} pb, and lies in the region being probed by direct detection experiments. The annihilation cross section peaks at $\phi_A = 3\pi/4$; notice that this value is not the point of maximal CP violation $\phi_A = \pi/2$.